Significant enhancements of nitrogen oxides, black carbon, and ozone in the North Atlantic lower free troposphere resulting from North American boreal wildfires

M. Val Martín,[1] R. E. Honrath,[1] R. C. Owen,[1] G. Pfister,[2] P. Fialho,[3] and F. Barata[3]

[1]   Extensive wildfires burned in northern North America during summer 2004, releasing large amounts of trace gases and aerosols into the atmosphere. Emissions from these wildfires frequently impacted the PICO-NARE station, a mountaintop site situated 6–15 days downwind from the fires in the Azores Islands. To assess the impacts of the boreal wildfire emissions on the levels of aerosol black carbon (BC), nitrogen oxides and O_3 downwind from North America, we analyzed measurements of CO, BC, total reactive nitrogen oxides (NO_y), NO_x ($NO + NO_2$) and O_3 made from June to September 2004 in combination with MOZART chemical transport model simulations. Long-range transport of boreal wildfire emissions resulted in large enhancements of CO, BC, NO_y and NO_x, with levels up to 250 ppbv, 665 ng m^{-3}, 1100 pptv and 135 pptv, respectively. Enhancement ratios relative to CO were variable in the plumes sampled, most likely because of variations in wildfire emissions and removal processes during transport. Analyses of $\Delta BC/\Delta CO$, $\Delta NO_y/\Delta CO$ and $\Delta NO_x/\Delta CO$ ratios indicate that NO_y and BC were on average efficiently exported in these plumes and suggest that decomposition of PAN to NO_x was a significant source of NO_x. High levels of NO_x suggest continuing formation of O_3 in these well-aged plumes. O_3 levels were also significantly enhanced in the plumes, reaching up to 75 ppbv. Analysis of $\Delta O_3/\Delta CO$ ratios showed distinct behaviors of O_3 in the plumes, which varied from significant to lower O_3 production. We identify several potential reasons for the complex effects of boreal wildfire emissions on O_3 and conclude that this behavior needs to be explored further in the future. These observations demonstrate that boreal wildfire emissions significantly contributed to the NO_x and O_3 budgets in the central North Atlantic lower free troposphere during summer 2004 and imply large-scale impacts on direct radiative forcing of the atmosphere and on tropospheric NO_x and O_3.

1.   Introduction

[2]   Boreal wildfires are large sources of reactive trace gases and aerosols in the atmosphere [e.g., *Goode et al.*, 2000; *Andreae and Merlet*, 2001]. The large amounts of trace gases and aerosols emitted by boreal forest fires are subject to long-range transport, with the potential to affect air quality on regional to global scales. Boreal wildfire plumes have been detected over continental [*Wotawa and Trainer*, 2000], intercontinental [*Forster et al.*, 2001; *Honrath et al.*, 2004], and even hemispheric [*Damoah et al.*, 2004] distances. It is recognized that boreal wildfires play an important role in the magnitude and interannual variability of tropospheric background CO in the Northern Hemisphere [e.g., *Novelli et al.*, 2003; *Edwards et al.*, 2004; *Kasischke et al.*, 2005]. Recent studies have also shown increased mean background summertime O_3 over northwestern North America [*Jaffe et al.*, 2004], the central North Atlantic [*Lapina et al.*, 2006] and Europe [*Simmonds et al.*, 2005] associated with fire emissions transport. This indicates that boreal wildfires may also impact background O_3.

[3]   Ozone plays an important role in the chemistry of the atmosphere since it is estimated to be the third most important greenhouse gas [*Houghton et al.*, 2001], and is the primary source of tropospheric hydroxyl radical. In addition, O_3 has negative impacts on ecosystems and human

---

[1]Department of Civil and Environmental Engineering, Michigan Technological University, Houghton, Michigan, USA.
[2]Atmospheric Chemistry Division, National Center for Atmospheric Research, Boulder, Colorado, USA.
[3]Group of Chemistry and Physics of the Atmosphere, University of the Azores, Terra Chã, Portugal.

health. Typically, tropospheric O$_3$ production in the Northern Hemisphere is driven by anthropogenic emissions. However, boreal wildfires are an important source of CO, NO$_x$ and nonmethane hydrocarbons (NMHC), resulting in the potential for significant formation of O$_3$ during the boreal fire season. Large-scale impacts of boreal fire emissions on tropospheric O$_3$ can occur as a result of dispersion of O$_3$ formed in boreal wildfire plumes. Alternatively, impacts on CO, NO$_x$ and NMHCs in the remote atmosphere could also lead to impacts on the O$_3$ budget over a large region.

[4] The magnitude of the resulting impact of boreal wildfire emissions on tropospheric ozone is not yet well quantified. Prior observations in boreal wildfire plumes indicate O$_3$ enhancements that range from very low in fresh plumes [e.g., *Goode et al.*, 2000; *Tanimoto et al.*, 2000] to low in moderately aged plumes [e.g., *Wofsy et al.*, 1992; *Mauzerall et al.*, 1996] to high in well-aged plumes [e.g., *Honrath et al.*, 2004; *Bertschi and Jaffe*, 2005]. Boreal wildfire emissions have a large degree of variability, and are a function of fuel type (e.g., peat fires versus crown fires) and/or burning conditions (e.g., smoldering versus flaming) [*Goode et al.*, 2000; *Kasischke et al.*, 2005]. This causes uncertainty and variability in the emissions of NO$_x$, a critical compound that controls O$_3$ production rate.

[5] Measurements of a number of reactive nitrogen species over the North American boreal region were made during the ABLE3A and ABLE3B campaigns. These studies showed that the reactive nitrogen distribution over this region was significantly affected by boreal wildfire emissions [e.g., *Sandholm et al.*, 1992; *Singh et al.*, 1994]. However, the photochemical O$_3$ production resulting from boreal wildfire NO$_x$ emissions was concluded to be a negligible source of O$_3$ over this region [*Jacob et al.*, 1992; *Mauzerall et al.*, 1996], because of a combination of low NO$_x$ emissions and low estimated total fire magnitude. However, these studies suggested that dispersion of PAN produced in the fire plumes may provide a major source of NO$_x$, particularly in warmer layers of the troposphere at low altitude [*Jacob et al.*, 1992; *Singh et al.*, 1994], and hence could contribute to O$_3$ production far downwind from the fires. Consistent with this expectation, *DeBell et al.* [2004] reported significant enhancements of NO$_y$ and O$_3$ at several surface sites over the eastern United States resulting from a Quebec boreal wildfire plume in July 2002. However, most of these measurements were made in the boundary layer, and loss of NO$_y$ and O$_3$ by surface deposition may have obscured the true magnitude of the fire plume aloft.

[6] In addition to trace gases, boreal wildfires emit large amounts of aerosol black carbon (BC), on average about 10% of the annual anthropogenic BC emissions in the Northern Hemisphere [*Bond et al.*, 2004]. Recently, it has been shown that BC emissions from boreal wildfires and anthropogenic sources can be efficiently transported to remote regions, such as the Arctic [*Stohl et al.*, 2006] and the northwestern Pacific region [*Park et al.*, 2005]. BC emissions are a significant factor in climate change because of their absorption of light in the atmosphere [*Hansen et al.*, 2000; *Bond and Sun*, 2005]. Therefore the export of BC far downwind from the source emissions may contribute to the radiative forcing of the atmosphere, and thereby affect climate.

[7] During summer 2004, extensive wildfires burned in Alaska (the largest area on record) and western Canada,

releasing large amounts of trace gases and aerosols into the atmosphere. For instance, CO emitted from mid-June to August was on the order of the anthropogenic CO emissions for the entire continental United States during that same time period [*Pfister et al.*, 2005; S. Turquety et al., Inventory of boreal fire emissions for North America in 2004: The importance of peat burning and pyroconvective injection, submitted to *Journal of Geophysical Research*, 2006, hereinafter referred to as Turquety et al., submitted manuscript, 2006]. Intense plumes of these boreal wildfires were observed over large regions of North America and Europe by research aircraft [*Flocke et al.*, 2005; *de Gouw et al.*, 2006; E. Real et al., Processes influencing ozone levels in Alaskan forest fires plumes during long-range transport over the North Atlantic, submitted to *Journal of Geophysical Research*, 2006, hereinafter referred to as Real et al., submitted manuscript, 2006] and at several sites over the Arctic [*Stohl et al.*, 2006] during the International Consortium for Atmospheric Research on Transport and Transformation (ICARTT) study [*Fehsenfeld et al.*, 2006].

[8] In this paper, we present measurements of the composition of highly aged plumes from these fires sampled in the North Atlantic lower free troposphere (FT), using measurements at the PICO-NARE station. Measurements of CO, BC, NO$_y$, NO$_x$ and O$_3$ made from June to early September 2004 are analyzed to assess the impact of boreal wildfires on levels of aerosol BC and nitrogen oxides (NO$_x$ and NO$_y$) over the central North Atlantic lower FT, to characterize the associated enhancements of O$_3$ in highly aged plumes, and to determine the resulting implications of the North American boreal wildfires for the regional and hemispheric NO$_x$ and O$_3$ budgets.

2. Experimental Methods

2.1. PICO-NARE Station

[9] Observations of CO, BC, NO$_x$, NO$_y$ and O$_3$ were made at the PICO-NARE observatory from June to September 2004. The PICO-NARE station is situated on the summit caldera of the inactive volcano Pico (altitude 2.2 km) in the Azores Islands, Portugal (38° N, 28°W). The Azores are frequently impacted by airflow from high latitudes, which can transport emissions from boreal wildfires in Canada, Alaska and Siberia, and bring them to the Azores 6 to 15 days later. The station is located in the lower FT since marine boundary layer heights in this region are typically less than 1 km during the summer. Upslope flow can transport air from lower altitudes to the mountaintop, including occasionally from the boundary layer. However, a detailed assessment of the impact of upslope flow to the station found that upslope flow affects the PICO-NARE station much less than it does many other mountain observatories, and on many summer days tropospheric air is sampled throughout the day [*Kleissl et al.*, 2006]. From June to September 2004, less than 25% of the time presented the meteorological conditions necessary for an air mass from below the mountain to reach the summit, i.e., weak synoptic winds and strong insolation for buoyant driven lifting or strong synoptic winds for mechanically driven lifting. Periods potentially affected by upslope flow were identified as described by *Kleissl et al.* [2006] and removed from the analysis. None of the periods discussed

in detail below contain data affected by upslope flow. Further details on the PICO-NARE station and the occurrence of upslope flow to the station are presented elsewhere [*Honrath et al.*, 2004; *Kleissl et al.*, 2006].

2.2. Measurements

2.2.1. Nitrogen Oxides

[10] NO, NO_2, and NO_y were determined by an automated $NO_{x,y}$ system developed at Michigan Technological University. This $NO_{x,y}$ system is an improved version of the instrument previously described by *Peterson and Honrath* [1999]. NO, NO_2, and NO_y were determined using established techniques: NO detection by O_3 chemiluminescence [*Ridley and Grahek*, 1990], NO_2 by conversion to NO via ultraviolet photodissociation [*Kley and McFarland*, 1980; *Parrish et al.*, 1990], and NO_y by Au-catalyzed reduction to NO in the presence of CO [*Bollinger et al.*, 1983; *Fahey et al.*, 1985]. The $NO_{x,y}$ system was operated on an automated cycle, which included twice daily NIST-traceable calibration with NO and NO_2, regular measurements of NO and NO_2 (twice per week) and NO_y (once per week) artifacts in zero air, and determination of the NO_y conversion efficiency in ambient air of two NO_y compounds (i-propyl nitrate and HNO_3) and one non-NO_y compound (CH_3CN). Measurements were recorded as 30-s averages (NO and NO_2) and 20-s averages (NO_y) every 10 min, and were further averaged to obtain the 30-min averages used in this work. Ambient NO_2 was determined by subtracting the signal due to ambient NO from the NO_2 instrument signal, and further multiplying this term by the NO_2 sensitivity [*Gao et al.*, 1994]. NO_x was calculated as the sum of the 30-s average measurements of NO and NO_2 during a single measurement cycle.

[11] Total uncertainty of the NO, NO_2 and NO_y measurements at low mixing ratios resulted from measurement precision and uncertainty in the instrument artifact correction, while measurement accuracy was the primary source of uncertainty at higher levels. The precision of individual measurements was mainly attributable to counting noise, which resulted from photon counting statistics. Excluding periods with high ambient variability, the precision (2-σ) of the 30-min averages was less than 6 pptv (median 5 pptv) for NO, less than 13 pptv (median 10 pptv) for NO_2, less than 14 pptv (median 10 pptv) for NO_x, and less than 9 pptv (median 6 pptv) for NO_y. Potential bias resulting from uncertainty in the artifact correction was estimated to be less than 2 pptv for NO, 4 pptv for NO_2, 4 pptv for NO_x and 2 pptv for NO_y. Measurement accuracy was estimated to be 4% on the basis of total uncertainty of the sample and calibration mass flow controllers and the NO standard calibration gas mixing ratio.

[12] Accuracy of the NO_y measurements also depends on the effective conversion of NO_y compounds and the lack of significant conversion of non-NO_y compounds [*Fahey et al.*, 1985; *Kliner et al.*, 1997; *Kondo et al.*, 1997], in addition to the accurate determination of the resulting NO. On the basis of results from standard addition tests and regular calibrations, the observed NO_y included 92–100% of the actual NO_2 level (typically 97–100%), with similar values expected for PAN [*Fahey et al.*, 1985], 70–100% of the actual HNO_3 level, and 80–100% of the actual i-propyl nitrate. Measurements of NO_y presented in this work were corrected for nonunity NO_y conversion by using the NO_2 conversion efficiencies measured at the system. A maximum correction of 8% was applied, and mainly affected the NO_y observations made from mid-July to mid-August when a degraded NO_y converter lowered the NO_2 conversion efficiency to 92–95%. A manual wet cleaning procedure was implemented in mid-August, and the NO_2 conversion efficiency was restored back to the expected value of 97–100%. In addition to the incomplete conversion of the NO_y species, this type of NO_y converter may overestimate true NO_y levels [*Fahey et al.*, 1985; *Kliner et al.*, 1997]. However, that was not a problem during this study. Interference from reduced nitrogen species (such as NH_4, HCN, and CH_3CN) was found to be always less than 0.3% during regular (twice daily) testing using standard addition of CH_3CN, a potential NO_y interferant present in biomass-burning plumes [*de Gouw et al.*, 2003]. This level of CH_3CN conversion in our system did not significantly contribute to the observations of NO_y gathered during boreal wildfire plumes: using the maximum enhancement of CH_3CN relative to CO (3.52 pptv CH_3CN/ppbv CO) in the boreal fire plumes intercepted by the NOAA WP-3 research aircraft during summer 2004 [*de Gouw et al.*, 2006], we estimate that the maximum impact of CH_3CN on the NO_y/CO enhancement ratios presented below is 0.01 pptv/ppbv CO, less than 0.2% of the lowest NO_y/CO enhancement ratio reported below.

[13] Observations of nitrogen oxides made during periods with near-calm winds and high ambient variability were also excluded from the analysis. This was done for two reasons. First, calm winds may lead to the removal of HNO_3 by deposition on the mountain surface. Therefore observations of NO_y during these periods may not be representative of the actual upwind NO_y levels. Second, unexpected spikes in ambient NO_x and NO_y were sometimes observed during low-wind periods (usually wind speeds less than 3 m/s), suggesting that a local source may have perturbed the measurements. On the basis of analysis of air sampled directly at several volcano vents (with NO_x reaching 1 to 8 ppbv), we deduce that volcanic emanations were the cause of the observed spikes. Therefore, to ensure that all the NO_x and NO_y observations were representative of free tropospheric air, we excluded (1) measurements made during low to calm winds (wind speed < 1 m/s), to avoid including NO_y observations with potential HNO_3 removed on the mountain surface, and (2) measurements with high ambient variability, to avoid including nitrogen oxides resulting from volcanic emissions. For this purpose, periods with high ambient variability were defined as those when the 30-min NO_x standard error was above 10 pptv or the 30-min NO_y standard error exceeded 10 pptv + 0.25([NO_y]−90), where the second term was included to allow increased variability during periods of high NO_y. The wind speed criterion removed 7% of the measurements during the study period, and the ambient variability screen removed an additional 23%.

2.2.2. CO and O_3

[14] CO was measured by a nondispersive infrared (NDIR) photometer (Thermo Environmental, Inc. (TEI), Model 48C-TL), modified as described by *Parrish et al.* [1994] and calibrated daily with a CO calibration gas referenced to the NOAA Global Monitoring Division

standard. The instrument alternated between two minutes of zero measurement and two minutes of ambient measurement; the first minute of each mode was discarded to ensure equilibration. O$_3$ was measured with a commercial ultraviolet absorption instrument (Thermo Environmental, Inc., Model 49C). The stability of the zero reading and the absence of O$_3$ loss in the inlet and line were confirmed on a daily basis. CO and O$_3$ data were recorded as one minute averages, and were further averaged to obtain the 30 minute averages used in this work. CO measurement uncertainty (2-σ) was estimated to be 7% on the basis of total uncertainty of the sample and calibration mass flow controllers and the CO calibration standard mixing ratio. The 30-min averages used in this work averaged seven to eight 1-min average points, and had a precision (2-σ) of 9 ppbv from June to mid-July, and 4 ppbv after mid-July. O$_3$ measurement precision (2-σ) was usually less than 1 ppbv, on the basis of the standard deviation of the thirty 1-min measurements included in each 30-min average. More details on the CO and O$_3$ instruments are presented by *Owen et al.* [2006] and *Honrath et al.* [2004].

2.2.3. Aerosol Black Carbon

[15] Measurements of aerosol light absorption at seven wavelengths (0.37, 0.47, 0.52, 0.59, 0.66, 0.88 and 0.95 μm) were conducted using an aethalometer (Magee Scientific, Model AE31). Briefly, this instrument determines the attenuation of light at these wavelengths transmitted through particles accumulated on a quartz filter, relative to a clean spot on the same filter. The change in attenuation as a function of time is used to determined the light absorption coefficient ($\sigma_{aerosol}$). The $\sigma_{aerosol}$ as a function of wavelength is analyzed to identify the presence of non-BC absorbing compounds [*Fialho et al.*, 2005] (none were significant during the period discussed here) and converted to equivalent BC using the calibration constant recommended by the manufacturer (14.6 μm m^2 g^{-1}). The equivalent BC values are referred to here as BC. The detection limit of the aethalometer depends mainly on the stability of the optics, filter spot area errors, flow rate uncertainties and time error, and was estimated to be 25 ng m^{-3} (2-σ) for the integration period of one hour. More details on the aethalometer used in this study and the approach used to determine the BC concentrations are presented elsewhere [*Fialho et al.*, 2005].

2.3. Model Simulations and Transport Analysis

[16] To identify periods apparently impacted by upwind boreal wildfire emissions, we examined CO mixing ratios simulated at the PICO-NARE station by the Model for OZone and Related Chemical Tracers (MOZART) global chemical transport model [*Horowitz et al.*, 2003]. MOZART simulations were driven by 6-hourly meteorological fields from the National Centers for Environmental Predictions (NCEP) National Center for Atmospheric Research reanalysis. The spatial resolution of the model is ~2.8° × 2.8° with 28 levels between the surface to 2 hPa. The chemical time step of the model is 20 minutes. Emissions of CO from the 2004 North American boreal wildfires were optimized to match MOPITT CO observations using an inverse modeling technique [*Pfister et al.*, 2005]. Boreal wildfire CO emissions were injected uniformly from 0 to 9 km. MOZART simulations used in this work are mixing ratios averaged over 2-hour intervals and interpolated to the

pressure and location of the PICO-NARE observatory [*Pfister et al.*, 2006]. To assess the magnitude of fire impact at the PICO-NARE station, we used the MOZART-simulated ratio of CO fire tracer (CO emitted from North American boreal wildfires) to total CO mixing ratio (i.e., [CO]$_{fire}$/[CO]$_{total}$) interpolated to the measurement times (hereinafter termed the "MOZART fire-CO fraction").

[17] A second MOZART tracer was used for U.S. anthropogenic CO emissions to evaluate the contribution of anthropogenic emissions during the fire-impacted observations. For this purpose, we used the MOZART-simulated ratio of U.S. anthropogenic CO tracer to total CO mixing ratio at the PICO-NARE station (i.e., [CO]$_{anthro}$/[CO]$_{total}$) interpolated to the 30-min average field observations (hereinafter termed the "MOZART anthro-CO fraction").

[18] To complement field observations and MOZART simulations, we used backward trajectories analysis. We calculated backward trajectories with the Hybrid Single-Particle Lagrangian Integrated Trajectories (HYSPLIT-4) model [*Draxler and Rolph*, 2003]. This model uses 6-hourly data from the NCEP global FNL meteorological data set. Ten-day backward trajectories were calculated every hour. At each hourly arrival time, six backward trajectories ending at six different locations near the PICO-NARE station were calculated: one centered at the station, four separated from the first by 1° latitude and longitude, and one below the station, at 2000 m.

3. Results and Discussion

[19] Time series of CO, BC, NO$_y$, NO$_x$ and O$_3$ measurements and MOZART fire-CO fraction at the PICO-NARE station from July to 5 September 2004 are shown in Figure 1. Frequent periods with elevated CO levels coinciding with maxima of MOZART fire-CO fraction are evident.

3.1. Identification of Fire-Impacted Periods

[20] Periods when the hourly average of CO was above 110 ppbv and the MOZART fire-CO fraction was above 0.1 were identified as potentially impacted by upwind boreal wildfire emissions. The CO value of 110 ppbv is well above typical background CO levels at the station and is approximately the maximum value observed in boreal region outflow in the absence of fires, as discussed in section 3.3.1 below. (Although we use 30-min averages of CO throughout the remainder of this work, for the purpose of identifying fire-impacted periods we used hourly averages of CO to smooth the CO measurements and compare them with the CO cutoff value.) The MOZART fire-CO fraction cutoff of 0.1 corresponds to approximately the 70th percentile of all model simulated values at the PICO-NARE station for summer 2004. Both of these cutoff values were designed to be conservative and, as a result, may omit some additional periods influenced by boreal wildfire emissions. For example, on 12 August 1200 UTC to 15 August 2300 UTC, an enhancement of MOZART fire-CO fraction above 0.1 was correlated with an increase in CO, but CO did not exceed the 110 ppbv cutoff value. Conversely, on 30 July 0700–1100 UTC, the hourly average CO increased to 135 ppbv while backward trajectories indicated transport from active fires, but the MOZART fire-CO fraction was lower than 0.07, likely as a result of the model spatial
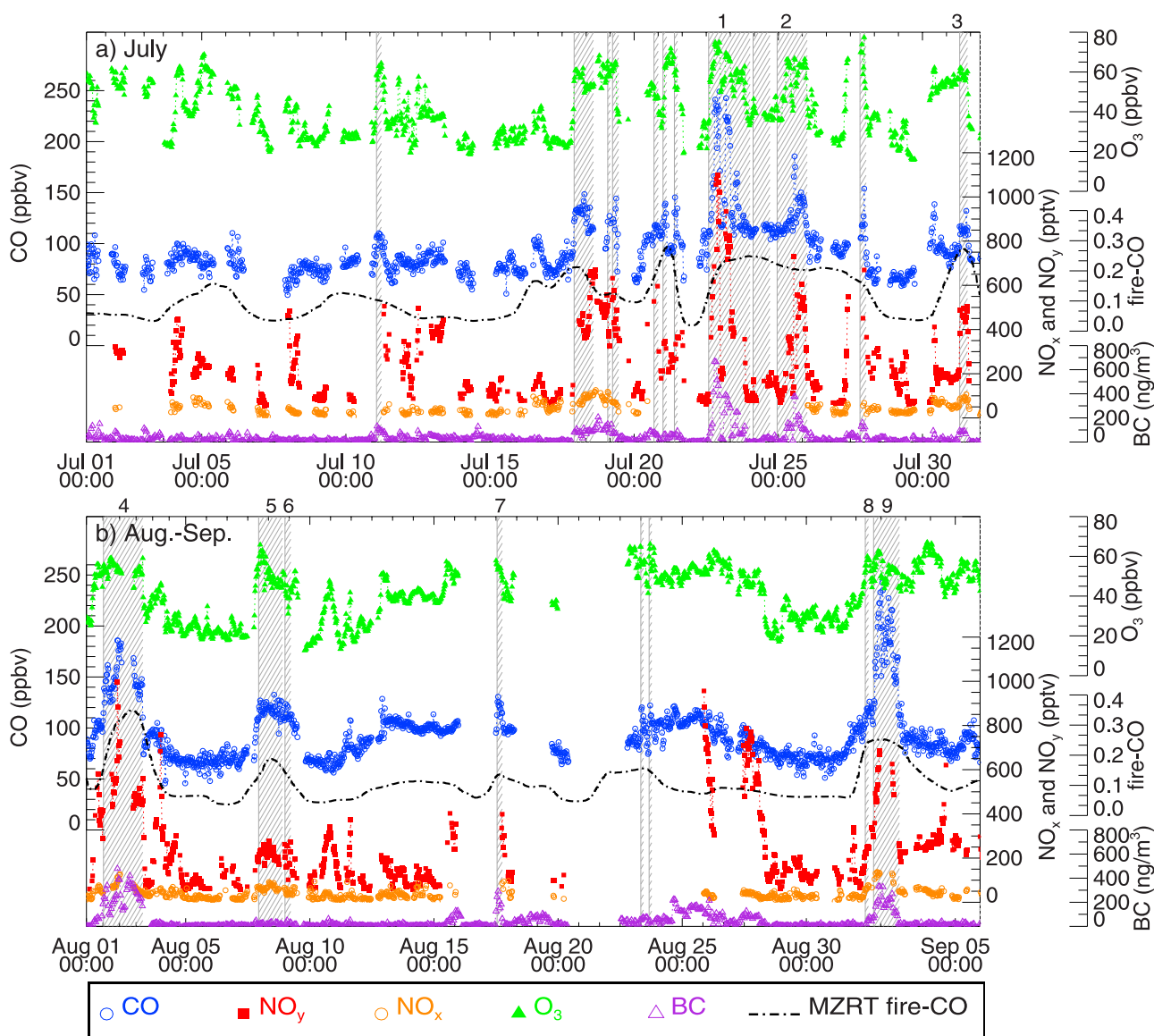
Figure 1. Summer 2004 time series of CO, BC, NO$_y$, NO$_x$ and O$_3$ measurements and MOZART fire-CO fraction at the PICO-NARE station. CO is plotted with open blue circles, NO$_y$ is plotted with red squares, NO$_x$ is plotted with open orange circles, BC is plotted with open purple triangles, O$_3$ is plotted with green triangles and MOZART fire-CO fraction is plotted with a dash-dotted line. Events identified as potentially boreal fire-impacted periods are identified with hatched areas; events further discussed in the text are numbered above the plot.

resolution. Although both of these cutoff values are somewhat arbitrarily selected, we find that the use of slightly larger or smaller cutoffs would not significantly affect the results presented below.

[21] In addition to outflow directly from the boreal regions, flow patterns that bring air to the Azores from higher latitudes can travel over the eastern United States [*Owen et al.*, 2006]. Therefore transport of boreal wildfire emissions over the Azores may be mixed with air potentially containing North American anthropogenic emissions, which can also be characterized by significant enhancements of CO and O$_3$ [*Honrath et al.*, 2004]. To determine the magnitude of the impact of anthropogenic emissions during the boreal wildfire periods, we use the MOZART anthro-CO fraction (not shown in Figure 1). According to

the MOZART simulations, anthropogenic emissions may explain some of the enhancements of CO at the station during summer 2004 either alone (e.g., 25 August, 0800–1900 UTC) or in combination with boreal wildfire emissions (e.g., 19 July, 0200–0900 UTC). To avoid inclusion of observations significantly affected by upwind anthropogenic emissions, we exclude from further analysis all observations with MOZART anthro-CO fraction values above 0.1. This MOZART anthro-CO fraction cutoff corresponded to approximately the 70th percentile of all model values simulated at the site.

[22] To better understand transport patterns during the periods identified as fire-impacted, we examined backward trajectories arriving at the PICO-NARE station altitude. Consistent with MOZART simulations, backward trajecto-

ries indicate transport of air that originated from the boreal regions in Alaska and/or Canada as shown in Figures 2a and 2b. However, the backward trajectories during a few periods indicated intermixing of subtropical and/or tropical air (hereinafter termed tropical air) with the boreal region outflow. Figure 2g shows an example of tropical backward trajectories intermixed with boreal region outflow. Observations made during these periods may be affected by clean tropical air and, thus, may not be representative of boreal region outflow. We identified periods potentially affected by tropical air when one or more backward trajectories originated over the Atlantic Ocean south of Pico Island (<35°N) and spent more than 90% of the time over the Atlantic Ocean before arriving at the site. We therefore omit all observations associated with tropical air intermixing from the analysis, with the following exception: during 23 July 0200–1800 UTC, although tropical air masses intermixed with boreal region outflow upwind the station, very large mixing ratios of CO recorded during most of the period ([CO] > 180 ppbv) indicate a lack of significant tropical air impact.

[23] Periods identified as potentially affected by boreal wildfire emissions on the basis of CO enhancements and MOZART fire-CO fraction criteria are identified with hatched areas in Figure 1; periods identified with the same criteria, but excluding periods of anthropogenic or tropical influence are also enumerated in Figure 1. Table 1 provides the statistics of the observations of CO, BC, NO$_y$, NO$_x$ and O$_3$ for both criteria, i.e., all fire-impacted observations and those excluding anthropogenic or tropical influence.

3.2. Overview of Summer 2004 Boreal Wildfire Observations

[24] The impact of boreal wildfire emissions at the PICO-NARE station was very frequent during summer 2004, as shown in Figure 1. A total of 21 events with apparent fire impact were identified during the period of study, accounting for 16% of the measurement time from 1 July to 5 September. Of these, 9 were unaffected by potential tropical or anthropogenic impacts. We focus only on these fire-impacted periods without anthropogenic or tropical influence, and refer to these periods as boreal wildfire events in the remainder of this paper. These 9 events are numbered in Figure 1. During these events, BC, NO$_y$, NO$_x$ and O$_3$ levels were also elevated and significantly correlated with CO in most of the cases. MOZART CO fire tracer ages calculated during the ICARTT study (10 July to 8 August) indicated the impact of North American fire emissions emitted 6 to 15 days earlier during the events identified during this period (i.e., events 1–5).

[25] Figures 3a and 3b show the time series of 30-min average observations of CO, NO$_y$, NO$_x$ and O$_3$, and 1-hour average observations of BC during 22–24 July and 1–2 September. These events, labeled respectively event 1 and event 9 in Figure 1, represent two of the most intense fire emission episodes observed during the study. Levels of CO, BC, NO$_y$ and O$_3$ during 22–24 July were extremely enhanced for more than a day, peaking at 249 ppbv, 665 ng m^{-3}, 1100 pptv and 75 ppbv, respectively. (NO$_x$ measurements were not available during this event.) This period had the highest level of CO yet recorded at the PICO-NARE station. Similarly, CO, BC, NO$_y$, NO$_x$ and O$_3$

levels were also strongly elevated for more than a day during 1–2 September, with peaks of 243 ppbv, 329 ng m^{-3}, 685 pptv, 134 pptv and 62 ppbv, respectively. The MOZART fire-CO fraction was also particularly high during these two events, as shown in Figure 1.

[26] Analyses of backward trajectories during events 1 and 9 confirm that the enhancements of these species occurred when airflow from Alaska and/or Canada arrived at the station. Examples of backward trajectories associated with the passage of the boreal fire plumes for these events are shown in Figures 2a and 2b. For comparison, Figures 2g and 2h show the airflow before the passage of each boreal fire plume. An important feature of these events is that the levels of these species remained constantly high for more than 24 hours, suggesting the impact of two very large highly aged plumes.

3.3. Impacts of Boreal Wildfire Emissions

[27] In this section, we assess the impacts of boreal wildfire emissions by comparing enhancements of CO, BC, NO$_y$, NO$_x$ and O$_3$ in fire-impacted boreal outflow to levels under similar conditions but in the absence of fires. First, however, we discuss the estimation of levels during periods of boreal outflow in the absence of fire emissions.

3.3.1. Estimation of Levels in Absence of Fires

[28] To estimate the background concentration at the PICO-NARE station in air from the fire source region, but in the absence of fire emissions, we identified two periods when boreal region outflow reached the station prior to the occurrence of the large fires: 7 June 0500–0900 UTC and 19 June 0800–1900 UTC. Early June was a period with low area burned over northern North America, and as a result, with low boreal wildfire emissions (Turquety et al., submitted manuscript, 2006). Therefore we expect that the contribution of boreal wildfire emissions to our site was small during these two periods. This is consistent with MOZART simulations, which indicate a maximum fire-CO fraction of 0.05 during these periods.

[29] Figure 3c shows the time series of 30-min average observations of CO and O$_3$ and 1-hour average observations of BC during the longer of these events, 19 June 0800–1900 UTC. (NO$_x$ and NO$_y$ measurements were not available at this time.) Examples of the backward trajectories associated with the passage of the air masses during and before this period are shown in Figures 2c and 2i, respectively. Average levels of CO, BC and O$_3$ during this period are used as background levels of these species for comparison with fire-impacted periods below. In addition, the maximum level of CO during this event (111 ppbv) was the basis for the 110 ppbv cutoff to select the boreal fire-impacted periods, as discussed in section 3.1. (The CO and O$_3$ background values used in this work are somewhat larger than the levels in nonfire air presented for the same data set by *Lapina et al.* [2006], because that analysis included periods with a mixture of boreal and nonboreal air).

[30] MOZART simulations during the other nonfire boreal outflow period indicate that anthropogenic emissions may have contributed to these observations (i.e., the MOZART anthro-CO fraction was above 0.1). However, nitrogen oxides measurements in non-fire-impacted boreal outflow were available only during the 7 June event. (Few measurements were available in June 2004 because of testing of the
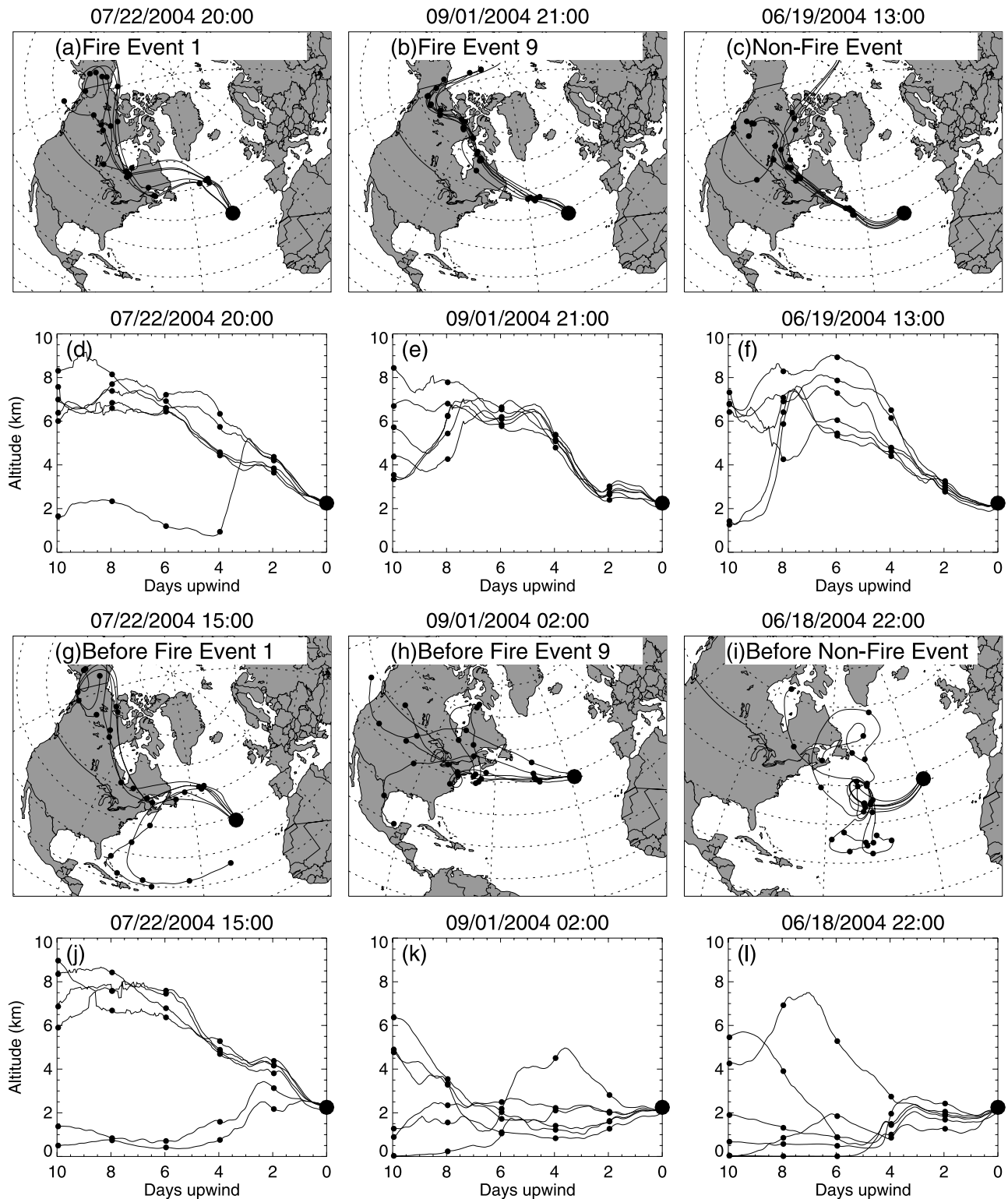
Figure 2. (a−c) Horizontal path of backward trajectories arriving at the measurement site during boreal region outflow for boreal region with upwind fire emissions (Figures 2a and 2b) and boreal region without upwind fire emissions (Figure 2c), along with (d−f) the altitude profile. (g−i) Horizontal path of backward trajectories before the passage of the boreal region air masses, along with (j−l) the altitude profile. Solid lines show the paths of the six trajectories ending on a grid around and below the station; trajectory arrival times are displayed above each pair of plots. Small dots indicate each 2 days travel time. The location of the PICO-NARE station is marked with a large dot.

Table 1. Comparison of CO, BC, NO$_y$, NO$_x$ and O$_3$ Levels During the Boreal Fire Events With Observations During Periods of Flow From Boreal Region in Absence of Fires and With All Observations During Summer 2004[a]

	Fire Observations[b]			Nonfire Observations[c]			Summer Observations[d]			
	Mean	Minimum–Maximum	N	Mean	Minimum–Maximum	N	Mean	Minimum–Maximum	Bckgrd[e]	N
CO, ppbv	139	107–249	379	100	92–111	23	93	46–249	77	3254
w/o anthro, trop air	144	108–249	277							
BC,[f] ng m^{-3}	133	<25–665	188	10	<25	11	38	<25–665	7	1705
w/o anthro, trop air	153	<25–665	133							
NO$_y$, pptv	389	71–1100	238	139	127–148	6	270	55–1380	143	1625
w/o anthro, trop air	406	71–1100	178							
NO$_x$, pptv	77	33–137	131	35	27–52	6	38	1–137	23	1525
w/o anthro, trop air	77	33–137	98							
O$_3$, ppbv	54	31–77	379	46	42–52	23	41	13–80	30	3428
w/o anthro, trop air	54	31–75	277							

[a]Reported are the average, minimum, maximum and number (N) of 30-min averages for CO, NO$_y$, NO$_x$ and O$_3$, and 1-hour averages for BC.

[b]Fire-impacted observations from July to 5 September. First row shows all fire-impacted observations; second row (w/o anthro, trop air) shows fire-impacted observations without anthropogenic or tropical air impact (see text for explanation).

[c]CO, BC and O$_3$ observations are from 19 June; NO$_y$ and NO$_x$ observations are from 7 June (see text for explanation).

[d]All observations from 1 June to 5 September 2004.

[e]Bckgrd: Background calculated as the 30th percentile of all summer 2004 observations.

[f]"<" indicates BC values below detection limit.

instruments prior the ICARTT campaign.) Average mixing ratios of NO$_y$ and NO$_x$ during this period were used as upper limit estimates of the background of these species in boreal region outflow in the absence of fires.

[31] The background levels of CO, BC, NO$_y$, NO$_x$ and O$_3$ used for boreal region outflow in the study are compared to background levels reported within the North American boreal region in Table 2. A wide range of background levels have been reported over the North American boreal region, reflecting differences in the latitude and altitude regions sampled, and the years of study. The values used here are similar to the background levels reported over the North American boreal region. The enhancement ratios calculated below are dependent on the background values used. This is discussed further in section 3.4.

3.3.2. Comparison of Levels in Boreal Region Outflow With and Without Fire Emissions

[32] Levels of CO, BC, NO$_y$, NO$_x$ and O$_3$ during boreal region outflow with fire emissions are summarized and compared to levels observed during boreal region outflow without fire emissions in Table 1. Statistics for all summertime observations are also shown. Average CO mixing ratios during the boreal wildfire events (144 ppbv) were above levels observed during flow from boreal region without fire emissions (100 ppbv), and were nearly double the summertime background (estimated as equal to the 30th percentile of all summertime measurements, 77 ppbv). This significant impact is consistent to what it has previously been observed at the PICO-NARE station [*Honrath et al.*, 2004; *Lapina et al.*, 2006], and for the entire Northern Hemisphere in years of high fire activity [e.g., *Novelli et al.*, 2003; *Edwards et al.*, 2004; *Kasischke et al.*, 2005].

[33] Levels of BC, NO$_y$, NO$_x$ and O$_3$ were also increased during the fire-impacted events, with levels of these species above those observed in boreal outflow in the absence of fires, and well above the typical summertime background at the site. For example, average NO$_x$ mixing ratios during the boreal wildfire events (77 pptv) were double those observed in boreal outflow without fire emissions (35 pptv) and triple the summertime background at the site (23 pptv).

[34] Figures 4a–4d show the relationships between CO (used as a tracer of fire emissions) and BC, NO$_y$, NO$_x$ and O$_3$. Solid color-coded symbols represent observations obtained during each boreal wildfire event, with one exception: grey circles represent the early June observations made in nonfire boreal outflow discussed in section 3.3.1. Most of the fire-impacted observations were above the background from the boreal regions in the absence of fires, consistent with the average difference noted above. In almost all events, these species were well correlated with CO, although distinct behaviors were observed depending on the levels of CO, in particular for O$_3$, as discussed further below.

[35] As discussed in section 3.1, a number of fire-impacted observations were excluded from the boreal wildfire events because of probable mixing of tropical air or MOZART-simulated anthropogenic emission transport. These observations are also shown in Figure 4: observations omitted because of tropical air mixing are represented with open cyan circles and those omitted because of anthropogenic emissions impact are represented with open black squares. Observations omitted because of tropical air mixing fall into two distinct groups of points, suggesting differing degrees of mixing. Of the observations excluded because of anthropogenic impact, some had exceptionally large NO$_y$, NO$_x$ and O$_3$ levels, suggesting significant anthropogenic impacts on those species as well. This impact is expect to be small in the events that were not excluded however. During those boreal wildfire events, MOZART-simulated anthropogenic CO was always below 7 ppbv, and usually (60% of the observations) below 3 ppbv.

3.4. Analysis of Enhancement Ratios in the Boreal Wildfire Plumes

[36] To characterize the amount of emitted BC and NO$_x$ that still remains in the plumes and the net O$_3$ production occurring in these plumes during transport to the station, we determined the enhancement ratio of BC, NO$_y$, NO$_x$ and O$_3$ with respect to CO during each boreal wildfire event [e.g., *Wofsy et al.*, 1992; *Stohl et al.*, 2002]. CO is commonly used as a tracer because it is emitted from combustion processes
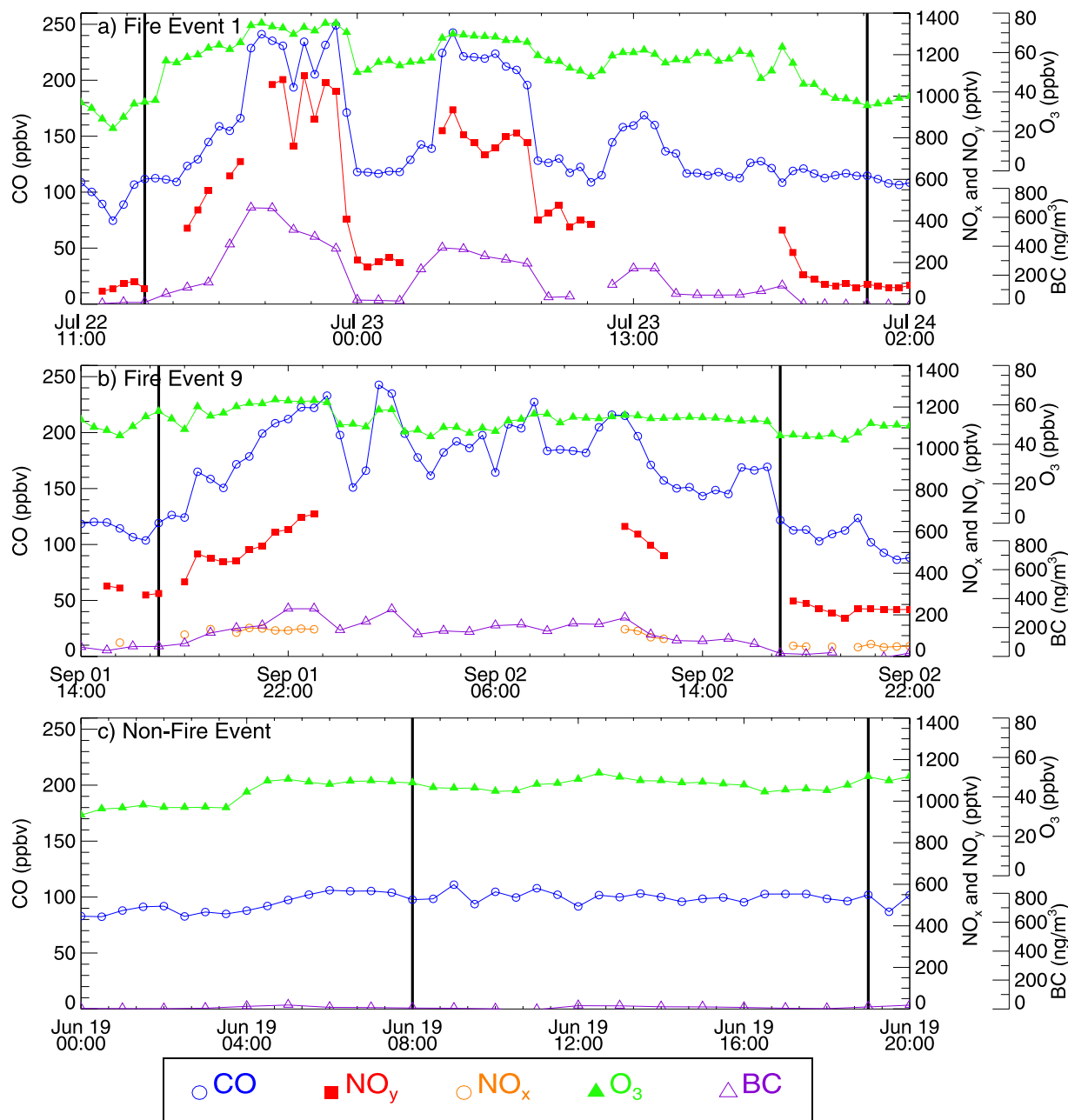
Figure 3. Time series of 30-min average CO, NO_x, NO_y and O_3, and 1-hour average BC observations during two boreal wildfire events and one boreal outflow period without upwind fire emissions: (a) fire event 1, 22 July 1800 UTC to 23 July 2100 UTC (NO_x measurements are not available); (b) fire event 9, 1 September 1630 UTC to 2 September 1600 UTC; and (c) nonfire event, 19 June 0800–1900 UTC (NO_x and NO_y measurements are not available). CO is plotted with open blue circles, NO_y is plotted with red squares, NO_x is plotted with open orange circles, BC is plotted with open purple triangles and O_3 is plotted with green triangles. Vertical solid lines indicate the start and end time of the event; remaining data are plotted to make the events more apparent.

in large quantities and has relatively a long lifetime [*Novelli et al.*, 1992]. We consider CO as an inert tracer in this approach. *de Gouw et al.* [2006], on the basis of analysis of volatile organic compound (VOC) measurements, indicated that OH concentrations in the boreal wildfire plumes intercepted by the NOAA WP-3 were four times smaller than typical values in the North Atlantic troposphere. Hence CO reaction with OH is expected to be limited in the boreal fire

plumes during the 6–15 days travel time to the station. We calculated mean values of ΔCO, ΔBC, ΔNO_y, ΔNO_x and ΔO_3 during each boreal wildfire event, and calculated enhancement ratios relative to CO for each event using these mean values. Here Δ indicates the difference between the concentration of the indicated species and the background concentration (e.g., $\Delta CO = [CO] - [CO]_{bkgd}$). Enhancement ratios are critically dependent on the background levels used

Table 2. Estimated Background Levels Over the North American Boreal Region[a]

Study	Period	Location	Altitude, km	CO, ppbv	NO$_y$, pptv	NO$_x$, pptv	O$_3$, ppbv	BC, ng m^{-3}
PICO-NARE[b]	Jun 2004	Pico, Azores	2.2	100	139	35	46	10
ABLE3A[c]	Jul–Aug 1988	Sub- and Arctic	<1–5.2	91–100	380–600	19–24	47–75[d]	n.r.
ABLE3B[e]	Jul–Aug 1990	eastern Canada	<1–6.2	80–110	164–542	21–35	25–65[d]	n.r.
Stohl06[f]	Jun–Aug 2004–2005	Summit, Greenland	3	n.r.	n.r.	n.r.	n.r.	20

[a]n.r., not reported.
[b]Mean values during boreal region outflow in June, used for background levels in enhancement ratio calculations (see text for explanation).
[c]Minimum and maximum values reported by *Sandholm et al.* [1992] and *Jacob et al.* [1992].
[d]Large range of O$_3$ reported reflects mainly O$_3$ dependence on altitude.
[e]Minimum and maximum values reported by *Talbot et al.* [1994], *Fan et al.* [1994], *Wofsy et al.* [1994], and *Mauzerall et al.* [1996].
[f]Median in summer 2004–2005 reported by *Stohl el al.* [2006].

[*Mauzerall et al.*, 1998]. Our background levels were derived using observations during transport events in June, as discussed in section 3.3.1. This results in background levels higher than those that would be estimated using clean marine levels or using the 30th percentile of all summertime measurements. This leads to reduced calculated enhancement ratios for all the species.

[37] Table 3 presents the resulting enhancement ratios. A large variability of enhancement ratios was observed. There are two causes that probably contributed to the varying enhancement ratios: different emission rates, which vary as a function of fuel type and burning conditions [*Goode et al.*, 2000; *Reid et al.*, 2005], and varying degrees of removal during transport. We examine both processes in the following sections.

3.4.1. Aerosol Black Carbon

[38] The relationships between BC and CO in boreal fire plumes and in background air from boreal regions are shown in Figure 4a. Estimated ΔBC/ΔCO ratios for each boreal fire event are shown in Table 3. Black carbon was significantly enhanced in all events relative to background from boreal outflow without upwind fire emissions, with the exception of events 5 and 6 (green diamonds and black squares in Figure 4a, respectively).

[39] A broad range of BC enhancement ratios (0.5–8.4 ng m^{-3}/ppbv; Table 3) were observed in the boreal fire plumes. Large variability in BC emissions from boreal wildfires has been reported previously. For example, BC concentrations during smoldering combustion are low, with BC mass fractions typically 2–5% of all carbon particles emitted, while BC mass fractions from flaming combustion are 4 to 28% of all carbon particles emitted [*Reid et al.*, 2005, and references therein].

[40] However, washout processes during transport to the station may also have contributed to this variability. To evaluate this possibility, we examined precipitation during transport and meteorological conditions at Pico during each event. For this purpose, we extracted rainfall rates from the HYSPLIT model output for the backward trajectories during each event and analyzed relative humidity measurements and archived photos of conditions at the station. Average rainfall rates were low (less than 0.05 mm/h) in all backward trajectories traveling from the boreal region to the station, with the exception of events 5, 6 and 9, which showed average rainfall rates of 0.09, 0.06 and 0.08 mm/h, respectively. (These events are represented by green diamonds, black squares and blue diamonds in Figure 4a, respectively.) Conditions at the station were dry and sunny during all events, with the exception of event 6, when heavy fog, and

most likely rain, was present. Therefore the lower ΔBC/ΔCO ratios during events 5, 6 and 9 compared to those during the other events are consistent with the wet scavenging of a greater fraction of BC during transport and/or at the station location during those events. This is consistent with previous observations of light absorbing aerosols (e.g., BC) in boreal fire plumes, which indicate that a large fraction of aerosols may be removed in the presence of rain and/or clouds [*Bertschi and Jaffe*, 2005; *Stohl et al.*, 2006].

[41] The BC enhancement ratios we report are 8–141% (average 59%, or 78% excluding events 5, 6 and 9) of the BC/CO emission ratio from extratropical forest fires (6 ± 3 ng m^{-3}/ppbv) recommended by *Andreae and Merlet* [2001]. (The value of 141% is not significantly different from 100%, considering the uncertainties of the measurements and the recommended value.) These observations indicate that an important fraction of the total BC emitted into the plumes we sampled was efficiently exported to the Azores, very far downwind from the fires. This underscores other recent work that has documented long-range impacts of the North American wildfire BC emissions [*Stohl et al.*, 2006; T. Duck et al., Transport of forest fire emissions from Alaska and the Yukon Territory to Nova Scotia during summer 2004, submitted to *Journal of Geophysical Research*, 2006]. Since BC effectively absorbs light in the atmosphere [*Hansen et al.*, 2000; *Bond and Sun*, 2005], this implies a potentially significant large-scale impact of boreal wildfire emissions on the direct radiative forcing over the Northern Hemisphere troposphere.

3.4.2. NO$_y$

[42] Figure 4b shows the relationship between NO$_y$ and CO in the boreal wildfire plumes and in background air from boreal regions without fire emissions. Table 3 provides the ΔNO$_y$/ΔCO ratios estimated for each boreal fire event. Nitrogen oxides were significantly enhanced in all the boreal fire plumes, relative to background levels.

[43] The NO$_y$ enhancement ratios were highly variable, however (4.2–22.1 pptv/ppbv; Table 3). In the previous section, we concluded that the variation in BC enhancement ratios could be the result of a combination of emission variation among fires and wet removal during transit to the station. Since NO$_x$ emissions also vary as a function of type of combustion [e.g., *Yokelson et al.*, 1996; *Goode et al.*, 2000] and a part of NO$_y$ (i.e., HNO$_3$) is susceptible to wet deposition, the same processes are expected to contribute to the variation of NO$_y$ enhancement ratios. Consistent with this expectation, the events with the lowest ΔBC/ΔCO ratios are also those with the lowest ΔNO$_y$/ΔCO ratios (i.e., events 5, 6 and 9). As a result, a plot of NO$_y$ versus BC is
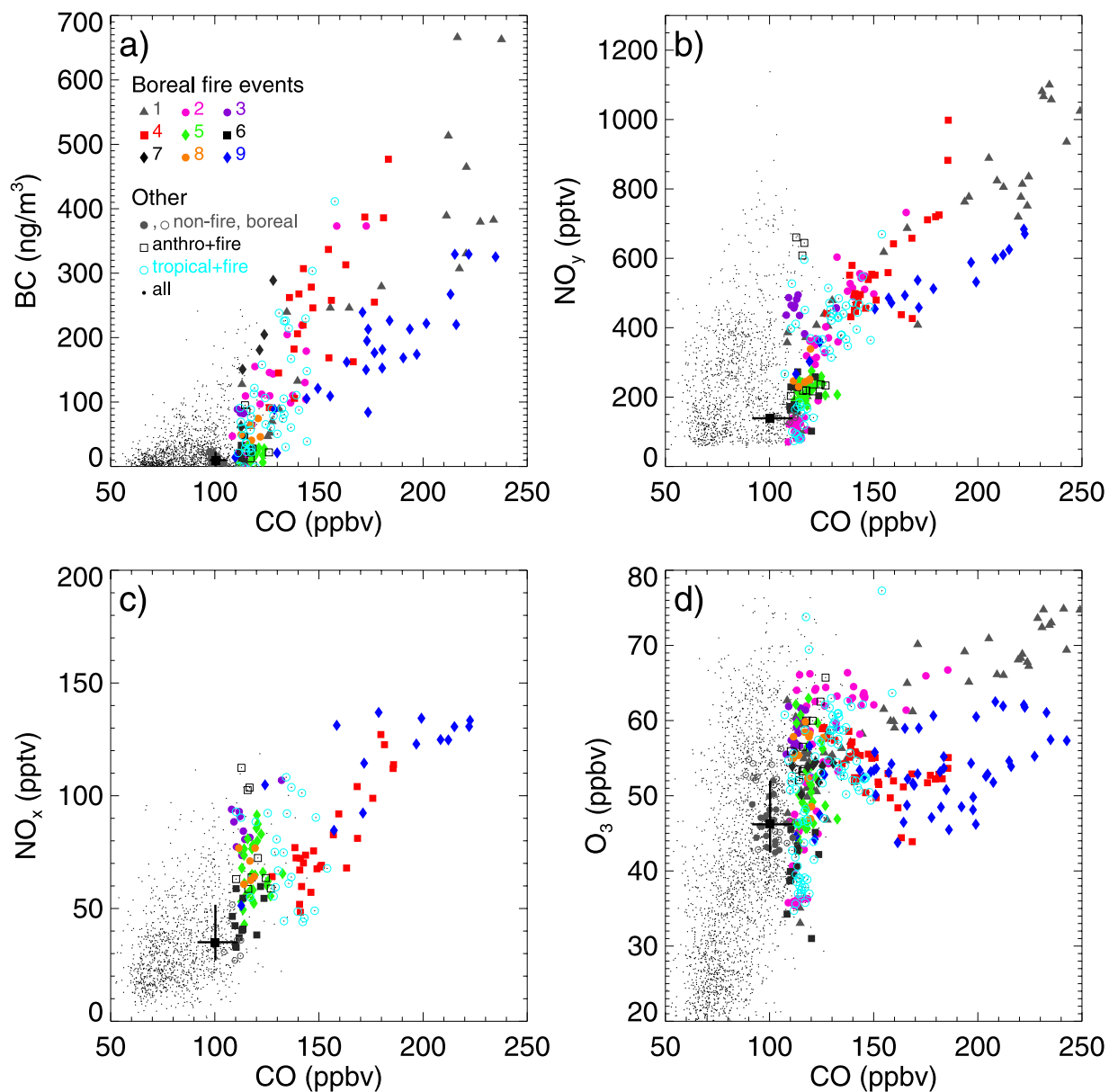
Figure 4. Relationship between CO and the indicated species during summer 2004: (a) BC versus CO, (b) NO$_y$ versus CO, (c) NO$_x$ versus CO and (d) O$_3$ versus CO. Boreal wildfire events listed in Table 3 and identified in Figure 1 are coded as follows: event 1 (dark grey triangles), event 2 (magenta circles), event 3 (purple circles), event 4 (red squares), event 5 (green diamonds), event 6 (black squares), event 7 (black diamonds), event 8 (orange circles) and event 9 (blue diamonds). Event 7 is not plotted for NO$_y$ and NO$_x$ because it contained fewer than 5 data points. Fire-impacted observations apparently impacted with tropical air are plotted with open cyan circles; fire-impacted observations apparently impacted with anthropogenic emissions are plotted with open black squares. Observations made during non-fire-impacted boreal outflow are plotted with small solid grey circles; non-fire-impacted boreal outflow observations with anthropogenic impact are plotted with open grey circles. The black square represents the average of non-fire-impacted boreal outflow observations, and black error bars connect minimum and maximum values observed. All other measurements during summer 2004 are plotted with small black dots.

less scattered than the plot of NO$_y$ versus CO, as shown in Figure 5, and the correlation of NO$_y$ with BC ($r^2 = 0.82$) is slightly better than that with CO ($r^2 = 0.75$). Additional evidence for efficient HNO$_3$ removal in some plumes is provided by aircraft measurements over the northwestern Atlantic Ocean, which found very low HNO$_3$ to NO$_y$ ratios in several 2004 North American fire plumes [*Flocke et al.*, 2005].

[44] Table 4 compares these ΔNO$_y$/ΔCO ratios to previous ΔNO$_y$/ΔCO ratios obtained from previous studies of boreal wildfire plumes. The mean enhancement ratio we observed (8 pptv/ppbv) is within the large range of mean

Table 3. Enhancement Ratios of the Species During the Boreal Wildfire Events Identified in Figure 1[a]

		$\Delta BC/\Delta CO$[b]		$\Delta NO_y/\Delta CO$[b]		$\Delta NO_x/\Delta CO$[b]		$\Delta O_3/\Delta CO$[b]	
Event	Period	ng m^{-3}/ppbv	N	pptv/ppbv	N	pptv/ppbv	N	ppbv/ppbv	N
1[c]	22 Jul 1800 UTC to 24 Jul 0000 UTC	3.60 ± 0.84	26	7.47 ± 1.08	35	NA	NA	0.23 ± 0.03	57
2	24 Jul 2300 UTC to 25 Jul 2330 UTC	3.72 ± 0.87	25	6.11 ± 1.09	41	NA	NA	0.31 ± 0.06	50
3	31 Jul 0700 UTC to 31 Jul 1300 UTC	4.91 ± 0.48	5	22.10 ± 2.62	10	3.63 ± 0.46	10	0.89 ± 0.11	13
4	1 Aug 1930 UTC to 3 Aug 0130 UTC	4.70 ± 0.55	20	8.10 ± 0.62	26	0.85 ± 0.08	25	0.14 ± 0.01	39
5	8 Aug 0130 UTC to 8 Aug 1730 UTC	0.47 ± 0.17	14	4.48 ± 0.32	29	1.73 ± 0.14	29	0.26 ± 0.06	33
6	9 Aug 0000 UTC to 9 Aug 0530 UTC	1.08 ± 0.42	6	4.17 ± 1.17	10	0.72 ± 0.22	12	−0.42 ± 0.10	12
7	17 Aug 1300 UTC to 17 Aug 1730 UTC	8.44 ± 2.26	5					0.37 ± 0.04	10
8	1 Sep 1000 UTC to 1 Sep 1500 UTC	2.50 ± 0.41	5	6.74 ± 0.79	7	1.92 ± 0.18	6	0.53 ± 0.08	11
9	1 Sep 1700 UTC to 2 Sep 1730 UTC	2.18 ± 0.28	25	4.67 ± 0.34	17	1.02 ± 0.07	14	0.09 ± 0.01	50

[a]NA, not available.

[b]Reported enhancement ratios (calculated as described in text), 2-σ uncertainty and number (N) of simultaneous 30-min average observations of NO$_y$, NO$_x$, O$_3$ and CO, and simultaneous 1-hour average observations of BC and CO. Events with N < 5 not shown.

[c]Event with apparent tropical air mixing impact.

values observed in plumes sampled over North America (5.6–14.1 pptv/ppbv; Table 4). The PICO-NARE mean enhancement ratio is also a significant fraction of the available (but poorly constrained) estimates of North American boreal fires NO$_x$/CO emission ratios, e.g., 12 pptv/ppbv [*Jain et al.*, 2006] or 26 ± 15 pptv/ppbv [*Andreae and Merlet*, 2001]. These comparisons indicate that a significant fraction of the NO$_x$ emitted into the sampled plumes was exported as NO$_y$ to the lower FT over the Azores region.

[45] This conclusion contrasts with some prior studies of the export of anthropogenic NO$_y$ to the FT, which conclude that a large majority of surface NO$_x$ emissions (>70%) is removed before or during export from the boundary layer during lofting mechanisms [e.g., *Liang et al.*, 1998; *Stohl et al.*, 2002; *Parrish et al.*, 2004; *Li et al.*, 2004].

[46] However, the boreal fire plumes sampled here differ from typical anthropogenic export in two key ways. First, in boreal wildfires PAN is expected to account for a significant fraction of NO$_y$ [*Jacob et al.*, 1992; *Singh et al.*, 1994] as a result of lower NO$_x$/hydrocarbon emission ratios [*Jacob et al.*, 1992]. Second, boreal wildfires can often be very energetic, releasing enough thermal energy to create smoke and convection columns that extend rapidly into the troposphere and even into the stratosphere [e.g., *Fromm et al.*, 2005; *Damoah et al.*, 2006]. The rapid vertical transport of emissions in fire-induced convection plumes soon after emission may contribute to the inefficient removal of NO$_y$ during the lofting mechanism, as has been suggested for BC [*Stohl et al.*, 2006]. In addition, as described above, most boreal fire plumes sampled at Pico were associated with low precipitation during transport as well as dry and sunny conditions at the site. Thus these conditions may have contributed to a more efficient export of NO$_y$.

3.4.3. NO$_x$

[47] Given the presumption of significant PAN content, the export of NO$_y$ is expected to lead to NO$_x$ release downwind from the fires. NO$_x$ mixing ratios were indeed significantly enhanced in these plumes relative to background. Figure 4c shows the relationship between NO$_x$ and CO in the boreal wildfire plumes and in background air from boreal regions in absence of fire emissions; $\Delta NO_x/\Delta CO$ ratios for the boreal wildfire events are listed in Table 3.

[48] The average of these NO$_x$ enhancement ratios (1.6 pptv/ppbv; Table 4) is significantly larger than those reported previously in moderately aged boreal fire plumes (0.2–0.7 pptv/ppbv; Table 4 [e.g., *Sandholm et al.*, 1992;

Mauzerall et al., 1996]). The occurrence of large enhancements of NO$_x$ and large $\Delta NO_x/\Delta CO$ ratios in these plumes implies that decomposition of PAN to NO$_x$, occurring as the plumes subside southward to the latitude of the Azores, may be an important source of NO$_x$ to the lower troposphere. This is consistent with the large enhancements of NO$_y$ observed at Pico as well as the large enhancements of NO$_y$ and PAN detected in plumes at higher altitudes than Pico over eastern North America [*Flocke et al.*, 2005] and over western Europe (H. Schlager, Deutsches Zentrum für Luft- und Raumfahrt (DLR), Germany, personal communication, 2006) during the ICARTT campaign.

[49] The overall impact of fire plumes on NO$_x$ levels during summer 2004 was significant. Fire emissions were responsible for 36% of all observations of NO$_x$ above 50 pptv (and 90% of all observations above 100 pptv). Fire plumes also led to a significant impact on NO levels. The 9 boreal wildfire events were responsible for 29% of all observations
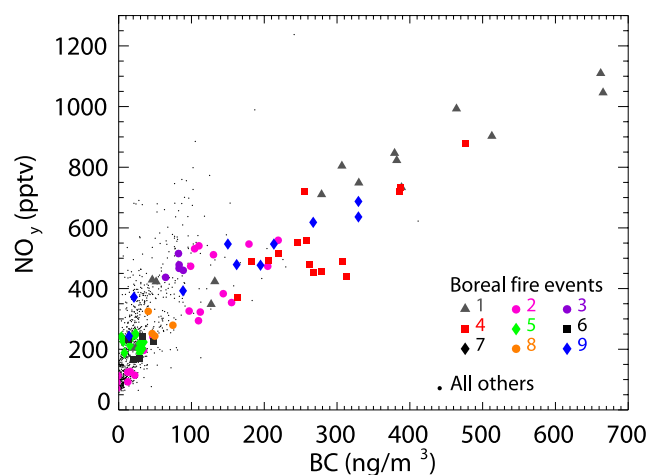

Figure 5. Relationship between BC and NO$_y$ during summer 2004. Boreal wildfire events are coded as follows: event 1 (dark grey triangles), event 2 (magenta circles), event 3 (purple circles), event 4 (red squares), event 5 (green diamonds), event 6 (black squares), event 8 (orange circles) and event 9 (blue diamonds). Event 7 contained <5 simultaneous data points and is not plotted. All other measurements during summer 2004 are plotted with small black dots.

Table 4. Enhancement Ratios of NO_y, NO_x and O_3 Relative to CO Observed in Boreal Fire Plumes[a]

Year	Fire Location	Sampling Location	Plume Height, km	Travel Time, day	$\Delta NO_y/\Delta CO$,[b] pptv/ppbv	$\Delta NO_x/\Delta CO$,[b] pptv/ppbv	$\Delta O_3/\Delta CO$,[b] ppbv/ppbv	Source
2004	AK, Can	Pico, Azores	2.2	6−15	8.0 (4.2−22.1)	1.6 (0.7−3.6)	0.2[c] (−0.4−0.9)	1
2002	Quebec, Can	eastern U.S.	0−2.5	1−3	4.1 (2.4−7.4)	n.r.	0.1 (0.01−0.09)	2
1990	Can, AK	eastern Can	1−6.2	<1	14.1 (2.5−37.8)	0.7 (0−3.8)	0.2 (0−0.7)	3
1988	Sib, AK, Can	AK, Can	1.5−6.1	near fire	10.9 (5.7−15.2)	0.2 (0−0.52)	0.35 (0.1−0.7)	4
1988	AK	AK	2.0−4.5	<1	5.6 (3.2−8.4)	n.r.	0.095 (0.014−0.18)	5
1997	AK	interior AK	1.6−1.8	∼2 hours	n.r.	n.r.	0−0.09	6
1998	eastern Sib	north Japan	<1	<1	n.r.	n.r.	0.01	7
1995	Can	south U.S.	0−3.0	2−4	n.r.	n.r.	0.11−0.17	8
2004	AK, Can	N Atl, W Eur	5−8	4−9	n.r.	n.r.	−0.01−0.08	9
2001−2003	Sib, AK, Can	Pico, Azores	2.2	6−15	n.r.	n.r	0.7 (0.4−0.9)	10
2002−2003	Sib	NW U.S/NE Pacific	0.7−5.0	7−10	n.r.	n.r.	0.4 (0.2−0.8)	11

[a]n.r., not reported; Can, Canada; AK, Alaska; Sib, Siberia; N Atl, North Atlantic; W Eur, western Europe.

[b]Reported average (minimum−maximum) in each measurement campaign (e.g., ABLE3B). Enhancement ratios were calculated using levels reported in background and biomass burning impacted air masses [e.g., *Sandholm et al.*, 1992] or extracted directly from reported enhancement ratios [e.g., *Wofsy et al.*, 1992]. References: 1, this work; 2, *DeBell et al.* [2004]; 3, ABLE3B [*Talbot et al.*, 1994; *Fan et al.*, 1994; *Mauzerall et al.*, 1996]; 4, ABLE3A [*Sandholm et al.*, 1992]; 5, ABLE3A [*Wofsy et al.*, 1992]; 6, *Goode et al.* [2000]; 7, *Tanimoto et al.* [2000]; 8, SOS-95 [*Wotawa and Trainer*, 2000; *McKeen et al.*, 2002]; 9, Real et al. (submitted manuscript, 2006); 10, PICO-NARE [*Honrath et al.*, 2004]; and 11, *Bertschi et al.* [2004] and *Bertschi and Jaffe* [2005].

[c]Average of high-CO-enhancement events 1, 2, 4 and 9, as discussed in section 3.4.4.

of NO above 20 pptv, and the average daytime fire-impacted NO was significantly larger (17 ± 2; mean ±2-σ) than the average daytime NO for all summer observations (11 ± 1). The large NO and NO_x mixing ratios present in these well-aged boreal wildfire plumes indicate a significant impact on the regional O_3 budget.

3.4.4. Ozone

[50] Figure 4d shows the relationship between O_3 and CO in the boreal wildfire plumes and in background air from boreal regions without fire emissions. The estimated O_3 enhancement ratio of each boreal fire event is provided in Table 3.

[51] The behaviors of O_3 in the fire plumes varied from significant O_3 enhancement in some plumes (e.g., event 1; grey triangles in Figure 4d) to O_3 enhancement relative to background, with a negative O_3−CO slope (e.g., event 4; red squares) to a smaller O_3 enhancement (e.g., event 9; blue diamonds). Furthermore, several fire plumes presented relatively large $\Delta O_3/\Delta CO$ ratios associated with only moderate CO enhancements (e.g., event 3; purple circles in Figure 4d; also events 5−8). The moderate CO enhancements during those periods make these events difficult to interpret, and therefore we focus here on the O_3 enhancement ratios in the high-CO-enhancement events.

[52] The significant enhancements of O_3 and large $\Delta O_3/\Delta CO$ ratios (mean 0.2 ppbv/ppbv) in these plumes are consistent with other studies that suggest that significant ozone production occurred downwind from boreal wildfires. For example, ozone enhancements of 20−30 ppbv were observed in boreal wildfire plumes after 5−7 days travel time to the southern United States [*Wotawa and Trainer*, 2000; *Morris et al.*, 2006] and to Europe [*Forster et al.*, 2001; Real et al., submitted manuscript, 2006]. Model simulations of the O_3 formation in biomass burning plumes indicate that the slow recycling of PAN, and to a lesser extend HNO_3 and organic nitrates, increases the effective lifetime of NO_x stimulating the continued formation of O_3 in these plumes beyond the typical 1-day NO_2 lifetime [*Chatfield and Delany*, 1990; Real et al., submitted manuscript, 2006].

[53] However, this mean $\Delta O_3/\Delta CO$ ratio is smaller than some reported previously and listed in Table 4 (e.g., 0.4−0.7 ppbv/ppbv [*Honrath et al.*, 2004; *Bertschi and Jaffe*, 2005; *Lapina et al.*, 2006]). This is mainly a result of the background value used here, as discussed in section 3.4. The average O_3 enhancement ratio we calculate increases to 0.3 ppbv/ppbv if the 2004 summertime background (Table 1) is used. If, in addition, all boreal wildfire events are considered, i.e., moderate- and high-CO-enhancement events, the average $\Delta O_3/\Delta CO$ ratio increases to 0.5 ppbv/ppbv (range 0.2−0.8 ppbv/ppbv).

[54] The significant O_3 enhancements observed during all but one event indicate O_3 production in most of the sampled boreal wildfire plumes. However, although O_3 levels were above background on average in all these events, the negative O_3−CO slope observed in event 4, and in parts of events 2 and 9, and the very low $\Delta O_3/\Delta CO$ ratio in parts of event 9 imply the removal of O_3 or the suppression of O_3 production as well. This behavior is not fully understood, but may be due to one or a combination of the following causes.

[55] First, a reduction of the O_3 production rates in the plumes would cause a low $\Delta O_3/\Delta CO$, but positive O_3−CO slope. A flat relationship between O_3 and CO, in combination with large enhancements of PAN and little NO_x [*Flocke et al.*, 2005] and large enhancements of VOCs [*de Gouw et al.*, 2006], was observed in some of the boreal fire plumes intercepted by the NOAA W-P3 at higher altitudes than Pico. *de Gouw et al.* [2006], on the basis of VOC measurements, deduced that OH levels were depressed in these plumes. Similar conditions (i.e., large enhancements of PAN and VOCs) were observed at the BAe146 (Real et al., submitted manuscript, 2006). As a consequence of low OH concentrations and limited NO_x availability, O_3 production rates may have been reduced. Similarly, *Pfister et al.* [2006] indicated that near the fire regions and, to a lesser extent downwind from the fires, O_3 production may also be reduced because of the combination of a reduction in the production rate and an increase in the loss rate of back-
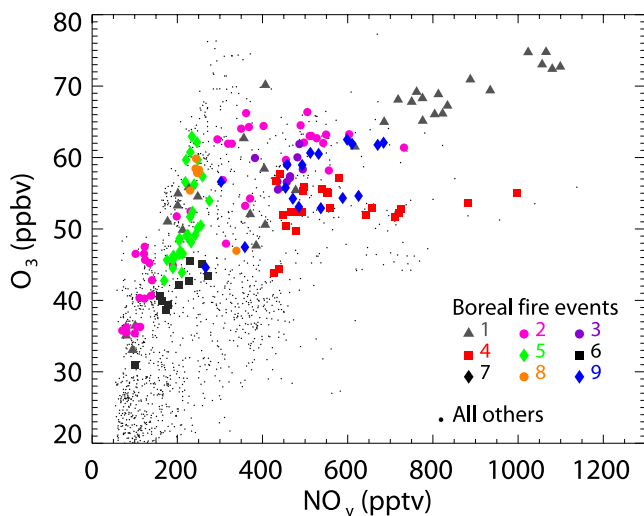
Figure 6. As Figure 5 but for the relationship between O$_3$ and NO$_y$.

ground O$_3$, as a result of a decrease in HO$_x$ (OH + HO$_2$) concentrations.

[56] Second, several studies have demonstrated the loss of O$_3$ by reaction with organic compounds present in aerosols [e.g., *de Gouw and Lovejoy*, 1998; *Griffin et al.*, 1999]. Biomass burning is a large source of smoke particles composed typically of organic carbon (OC) ~50–60% and BC ~5–10% [*Reid et al.*, 2005]. Given the significant levels of BC observed in the boreal fire plumes and the large ratio of OC to BC in biomass burning [*Reid et al.*, 2005], O$_3$ destruction on organic aerosols may have contributed to the reduced O$_3$ enhancement ratio or the negative O$_3$−CO relationship observed in some events.

[57] Finally, nighttime chemistry processes may also result in destruction of O$_3$. At night, chemical processing of NO$_x$ oxidizes NO$_x$ to HNO$_3$ via rapid heterogeneous hydrolysis of N$_2$O$_5$ in aerosols and initiates nocturnal oxidation of VOCs, with the concurrent destruction of O$_3$ [*Parrish et al.*, 1998; *Brown et al.*, 2006]. Thus nocturnal NO$_x$ emissions from boreal wildfires may result in a reduction of O$_3$ and NO$_y$, and result in reduced ΔO$_3$/ΔCO ratio or negative O$_3$−CO relationships.

[58] To further investigate the photochemical properties of the plumes, we present the relationship between O$_3$ and NO$_y$ in Figure 6. With the exception of event 4, O$_3$ and NO$_y$ showed positive correlations in all plumes ($r^2 = 0.5$–0.8). Positive O$_3$−NO$_y$ correlations are consistent with our expectation of photochemical O$_3$ production in the plumes, as a result of decomposition of PAN to NO$_x$ occurring in the air masses during subsidence to the station. The sole exception, event 4 (red squares) exhibits no correlation between O$_3$ and NO$_y$ (Figure 6) and a negative O$_3$−CO relationship (Figure 4d) and a larger BC-NO$_y$ relationship than the general trend (Figure 5). This situation suggests O$_3$ destruction from organic aerosols during transport toward the station. However, the data available here are insufficient to test this hypothesis.

[59] Finally, we have evaluated the possibility that stratospheric O$_3$ contributed to the O$_3$ enhancements observed during some of these events. Stratospheric O$_3$ frequently impacted the FT over eastern North America during summer 2004 (A. Thompson et al., IONS-04: New perspective on summertime UT/LS ozone over northeastern North America, submitted to *Journal of Geophysical Research*, 2006). Boreal fire plumes that impacted Pico were often associated with subsidence from altitudes of approximately 6–8 km, suggesting a potential stratospheric impact. To assess this, we used FLEXPART stratospheric O$_3$ tracer values simulated at the station location and altitude during 1 July to 16 August (A. Stohl, Norwegian Institute for Air Research (NILU), personal communication, 2006). Detailed information about the FLEXPART model is present elsewhere [*Stohl et al.*, 2005]. This analysis indicated that stratospheric O$_3$ occasionally impacted the station during the ICARTT period, but that the overall impact of stratospheric O$_3$ was rather small: the average (± standard deviation) of all stratospheric O$_3$ tracer values was 8.4 ± 5.2 ppbv. During the fire-impacted events, stratospheric O$_3$ tracer values were usually reduced, rather than increased, with an average (± standard deviation) of 5.8 ± 4.2 ppbv. We found only one episode during the boreal fire events (7 August 2300 UTC to 8 August 2100 UTC) when the stratospheric O$_3$ tracer was large (10 to 18 ppbv). This episode occurred during event 5 (green diamonds in Figure 4d). Even during this episode, the O$_3$ enhancement during the event did not appear to be due to stratospheric O$_3$, as FLEXPART stratospheric O$_3$ tracer values did not increase relative to values before or after the event. Therefore we conclude that stratospheric O$_3$ was not the cause of the enhancements of O$_3$ observed during event 5, and that the overall impact of stratospheric O$_3$ was not significant during the boreal fire plumes analyzed in the study.

3.5. Implications of Boreal Wildfires for the NO$_x$ and O$_3$ Budgets

[60] The NO$_y$ enhancement ratios observed at Pico may be used to estimate the total amount of NO$_x$ emitted from the fires and exported in the plumes by multiplying the observed NO$_y$/CO enhancement ratio by the fire CO emissions [*Stohl et al.*, 2002; *Parrish et al.*, 2004]. *Pfister et al.* [2005] estimated that 30 ± 5 Tg CO were emitted over the North American boreal region from mid-June to August, 2004, consistent with the estimate of Turquety et al. (submitted manuscript, 2006). Using the ΔNO$_y$/ΔCO ratio at the PICO-NARE station (8.0 pptv/ppbv CO; Table 4) as an approximation of the impact of long-range-transported fire emissions, this CO emission implies that the fires contributed 0.12 Tg NO$_y$ (as N). If, instead, we use total boreal fire CO emissions in a typical year (~61 Tg CO; [*Kasischke et al.*, 2005]), i.e., including Siberian emissions as well as North American, the total contribution to long-range-transported NO$_y$ is estimated as 0.24 Tg. These values are quite large. For comparison, the amount of eastern North American NO$_x$ emissions exported to the FT during mid-June through August 2004 was approximately 0.30 Tg NO$_y$ (as N). (This estimate is based on eastern U.S. NO$_x$ emissions equal to two thirds of the U.S. national emissions during that period, using total NO$_x$ U.S. emissions in 1999 reported by *Parrish et al.* [2004], adjusted for the 8.8% per year decrease of the on-road CO:NO$_y$ emission ratio, and estimated efficiency of export to the FT equal to approximately 25% during summertime [e.g., *Liang et al.*, 1998;

Stohl et al., 2002; *Parrish et al.*, 2004; *Li et al.*, 2004].) These observations imply significant impacts of the boreal wildfires on the NO_y budget over downwind regions distant from the fires.

[61] If the O_3 enhancement ratio at the PICO-NARE station applies to all fire emissions, the average $\Delta O_3/\Delta CO$ ratio (0.2 ppbv/ppbv), combined with the total CO emitted from the North American wildfires (30 Tg) or with the typical CO emitted from boreal wildfires (61 Tg), indicates that the boreal wildfires may have resulted in a source of $10-21$ Tg of O_3 during summer 2004. This method is generally consistent with the MOZART analysis of fire-induced O_3 production discussed by *Pfister et al.* [2006]. The monthly mean of our estimate ($4-8$ Tg O_3/month from mid-June to August) is $10-20\%$ of the July net photochemical O_3 production in the northern middle and high latitudes ($30-90°$ N; surface to 350 hPa) estimated by *Emmons et al.* [2003]. The ultimate impact could be even larger, since additional O_3 is expected to form as a result of the NO_x and PAN still remaining in the transported plumes. Therefore our observations indicate that boreal wildfires may significantly impact the hemispheric O_3 budget during the fire season.

[62] Given the current uncertainties in the CO emissions from boreal wildfires, the increase in dry and warm conditions over the boreal region [*Hassol*, 2004], and the increase in human-ignited fires [*Mollicone et al.*, 2006], most likely the impact of boreal wildfires is significantly larger than previously believed.

4. Conclusions

[63] North American boreal wildfire emissions frequently impacted the PICO-NARE station during summer 2004. Using MOZART simulations and enhancements of CO levels, we identified 21 events of long-range transport of boreal wildfire emissions to the site, which accounted for 16% of the time from 1 July to 5 September 2004. Fire-impacted boreal region outflow resulted in extremely high levels of CO, BC and nitrogen oxides, relative to other observations at the station, along with significant enhancements of O_3. Analysis of CO, BC, NO_y, NO_x and O_3 observations during the boreal wildfire events showed that levels of all these species were above those in background air from similar outflow in the absence of fires, and well above typical summertime background levels at the site. This indicates a significant contribution from the North American wildfire emissions to background levels of these species over the North Atlantic region during summer 2004.

[64] Enhancement ratios relative to CO were somewhat variable, however. This is attributed to a combination of variation of fire types and emissions and removal during transport to the site. Analyses of $\Delta BC/\Delta CO$ and $\Delta NO_y/\Delta CO$ indicated that a significant fraction of BC and NO_y resulting from the fires was scavenged in some plumes, but on average BC and NO_y were efficiently exported to the lower FT over the North Atlantic region. Analyses of $\Delta NO_x/\Delta CO$ ratios suggested that decomposition of PAN to NO_x, occurring as the plumes subside southward to the Azores, was an important source of NO_x. High levels of NO and NO_x imply continuing O_3 formation in these highly aged plumes.

[65] Ozone levels were also significantly enhanced. Analysis of $\Delta O_3/\Delta CO$ ratios indicated a varying behavior from plume to plume, with significant to moderate O_3 production, and included negative O_3-CO slopes in some plumes. We discussed several mechanisms that may have contributed to the complex behavior of O_3 in the fire plumes, and suggest that further work is needed to better understand this effect. However, the O_3 enhancements present in all but one plume indicate that significant photochemical production occurred during transport, most likely as a result of decomposition of PAN to NO_x. Lower O_3 production in other plumes may have resulted from a reduction in the O_3 production rates due to reduced OH concentrations and limited NO_x, or from destruction of O_3 during transport due to reaction with organic aerosols or nighttime chemistry.

[66] Our analyses demonstrate that boreal wildfire emissions can result in a significant source of BC, NO_x and O_3 in the central North Atlantic lower FT. Since our observations were made very far downwind from the fires, this suggests very large-scale impacts of boreal wildfires both on direct radiative forcing by BC and on tropospheric NO_x and O_3 budgets. Recent studies have shown a positive trend in the amount of areas burned over recent decades [*Gillett et al.*, 2004; *Kasischke and Turetsky*, 2006], likely as a result of warmer and drier conditions in the boreal region [*Hassol*, 2004], and possibly in combination with direct human impacts [*Mollicone et al.*, 2006]. Global Circulation Models predict more frequent and more severe fires as the climate changes [*Stocks et al.*, 1998; *Flannigan et al.*, 2000]. Thus the impact of boreal wildfires may become even more important in the near future.

References

Andreae, M., and P. Merlet (2001), Emissions from trace gases and aerosols from biomass burning, *Global Biogeochem. Cycles*, *15*, 955–966.

Bertschi, I. T., and D. A. Jaffe (2005), Long-range transport of ozone, carbon monoxide, and aerosols to the NE Pacific troposphere during the summer of 2003: Observations of smoke plumes from Asian boreal fires, *J. Geophys. Res.*, *110*, D05303, doi:10.1029/2004JD005135.

Bertschi, I. T., D. A. Jaffe, L. Jaegl, H. U. Price, and J. B. Dennison (2004), PHOBEA/ITCT 2002 airborne observations of transpacific transport of ozone, CO, volatile organic compounds, and aerosols to the northeast Pacific: Impacts of Asian anthropogenic and Siberian boreal fire emissions, *J. Geophys. Res.*, *109*, D23S12, doi:10.1029/2003JD004328.

Bollinger, M. J., R. E. Sievers, D. W. Fahey, and F. C. Fehsenfeld (1983), Conversion of nitrogen dioxide, nitric acid, and n-propyl nitrate to nitric oxide by gold-catalyzed reduction with carbon monoxide, *Anal. Chem.*, *55*, 1980–1986.

Bond, T. C., and H. Sun (2005), Can reducing black carbon emissions counteract global warming?, *Environ. Sci. Technol.*, *39*, 5921–5926, doi:10.1021/es0480421.

Bond, T. C., D. G. Streets, K. F. Yarber, S. M. Nelson, J.-H. Woo, and Z. Klimont (2004), A technology-based global inventory of black and

organic carbon emissions from combustion, *J. Geophys. Res.*, *109*, D14203, doi:10.1029/2003JD003697.

Brown, S. S., et al. (2006), Variability in nocturnal nitrogen oxide processing and its role in regional air quality, *Science*, *311*(5757), 67–70, doi:10.1126/science.1120120.

Chatfield, R. B., and A. C. Delany (1990), Convection links biomass burning to increased tropical ozone: However, models will tend to overpredict O$_3$, *J. Geophys. Res.*, *95*, 18,473–18,488.

Damoah, R., N. Spichtinger, C. Forster, P. James, I. Mattis, U. Wandinger, S. Beirle, T. Wagner, and A. Stohl (2004), Around the world in 17 days—Hemispheric-scale transport of forest fire smoke from Russia in May 2003, *Atmos. Chem. Phys.*, *4*, 1449–1471.

Damoah, R., et al. (2006), A case study of pyro-convection using transport model and remote sensing data, *Atmos. Chem. Phys.*, *6*, 173–185.

DeBell, L. J., R. W. Talbot, J. E. Dibb, J. W. Munger, E. V. Fischer, and S. E. Frolking (2004), A major regional air pollution event in the northeastern United States caused by extensive forest fires in Quebec, Canada, *J. Geophys. Res.*, *109*, D19305, doi:10.1029/2004JD004840.

de Gouw, J. A., and E. R. Lovejoy (1998), Reactive uptake of ozone by liquid organic compounds, *Geophys. Res. Lett*, *25*(6), 931–934.

de Gouw, J. A., C. Warneke, D. D. Parrish, J. S. Holloway, M. Trainer, and F. C. Fehsenfeld (2003), Emission sources and ocean uptake of acetonitrile (CH$_3$CN) in the atmosphere, *J. Geophys. Res.*, *108*(D11), 4329, doi:10.1029/2002JD002897.

de Gouw, J. A., et al. (2006), Volatile organic compounds composition of merged and aged forest fire plumes from Alaska and western Canada, *J. Geophys. Res.*, *111*, D10303, doi:10.1029/2005JD006175.

Draxler, R., and G. Rolph (2003), HYSPLIT4 model (HYbrid Single-Particle Lagrangian Integrated Trajectory) model, NOAA Air Resour. Lab., Silver Spring, Md. (Available at http://www.arl.noaa.gov/ready/hysplit4.html)

Edwards, D. P., et al. (2004), Observations of carbon monoxide and aerosols from the Terra satellite: Northern Hemisphere variability, *J. Geophys. Res.*, *109*, D24202, doi:10.1029/2004JD004727.

Emmons, L. K., et al. (2003), Budget of tropospheric ozone during TOPSE from two chemical transport models, *J. Geophys. Res.*, *108*(D8), 8372, doi:10.1029/2002JD002665.

Fahey, D. W., C. S. Eubank, G. Hubler, and F. C. Fehsenfeld (1985), Evaluation of a catalytic reduction technique for the measurement of total reactive odd-nitrogen NO$_y$ in the atmosphere, *J. Atmos. Chem.*, *3*, 435–468.

Fan, S., et al. (1994), Origin of tropospheric NO$_x$ over subarctic eastern Canada in summer, *J. Geophys. Res*, *99*(D8), 16,867–16,878.

Fehsenfeld, F., et al. (2006), International Consortium for Atmospheric Research on Transport and Transformation (ICARTT): North America to Europe: Overview of the 2004 summer field study, *J. Geophys. Res.*, doi:10.1029/2006JD007829, in press.

Fialho, P., A. D. A. Hansen, and R. E. Honrath (2005), Absorption coefficients by aerosols in remote areas: A new approach to decouple dust and black carbon absorption coefficients using seven-wavelength aethalometer data, *J. Aerosol Sci.*, *36*, 267–282.

Flannigan, M., B. Stocks, and B. Wotton (2000), Climate change and forest fires, *Sci. Total Environ.*, *262*, 221–229.

Flocke, F., et al. (2005), Results from fast airborne measurements of PANs during the 2004 New England Air Quality Study, *Eos Trans. AGU*, *86*(52), Fall Meet. Suppl., Abstract A54C-03.

Forster, C., et al. (2001), Transport of boreal forest fire emissions from Canada to Europe, *J. Geophys. Res.*, *106*, 22,887–22,906.

Fromm, M., R. Bevilacqua, R. Servranckx, J. Rosen, J.P. Thayer, J. Herman, and D. Larko (2005), Pyro-cumulonimbus injection of smoke to the stratosphere: Observations and impact of a super blowup in northwestern Canada on 3–4 August 1998, *J. Geophys. Res.*, *110*, D08205, doi:10.1029/2004JD005350.

Gao, R. S., E. R. Keim, E. L. Woodbridge, S. J. Cicora, M. H. Proffitt, T. L. Thompson, R. J. Mclaughlin, and D. W. Fahey (1994), New photolysis system for NO$_2$ measurements in the lower stratosphere, *J. Geophys. Res.*, *99*, 20,673–20,681.

Gillett, N., A. J. Weaver, F. W. Zwiers, and M. D. Flannigan (2004), Detecting the effect of climate change on Canadian forest fires, *Geophys. Res. Lett.*, *31*, L18211, doi:10.1029/2004GL020876.

Goode, J. G., R. J. Yokelson, D. E. Ward, R. A. Susott, R. E. Babbitt, M. A. Davies, and W. M. Hao (2000), Measurements of excess O$_3$, CO$_2$, CH$_4$, C$_2$H$_4$, C$_2$H$_2$, HCN, NO, NH$_3$, HCOOH, CH$_3$COOH, HCHO, and CH$_3$H in 1997 Alaskan biomass burning plumes by airborne Fourier transform infrared spectroscopy (AFTIR) [O$_3$ CO$_2$ CH$_4$ C$_2$H$_4$ C$_2$H$_2$ NH$_3$ CH$_3$COOH CH$_3$H], *J. Geophys. Res.*, *105*(D17), 22,147–22,166.

Griffin, R. J., III, R. C. Flagan, and J. H. Seinfeld (1999), Organic aerosol formation from the oxidation of biogenic hydrocarbons, *J. Geophys. Res.*, *104*(D3), 3555–3568.

Hansen, J., M. Sato, R. Ruedy, A. Lacis, and V. Oinas (2000), Global warming in the twenty-first century: An alternative scenario, *Proc. Natl. Acad. Sci. U.S.A.*, *97*, 9875–9880.

Hassol, S. J. (2004), *Impacts of a Warming Arctic: Arctic Climate Impact Assessment*, Cambridge Univ. Press, New York.

Honrath, R. E., R. C. Owen, M. Val Martín, J. S. Reid, K. Lapina, P. Fialho, M. P. Dziobak, J. Kleissl, and D. L. Westphal (2004), Regional and hemispheric impacts of anthropogenic and biomass burning emissions on summertime CO and O$_3$ in the North Atlantic lower free troposphere, *J. Geophys. Res.*, *109*, D24310, doi:10.1029/2004JD005147.

Horowitz, L. W., et al. (2003), A global simulation of tropospheric ozone and related tracers: Description and evaluation of MOZART, version 2, *J. Geophys. Res.*, *108*(D24), 4784, doi:10.1029/2002JD002853.

Houghton, J. T., Y. Ding, D. J. Griggs, M. Noguer, P. J. van der Linden, X. Dai, K. Maskell, and C. A. Johnson (Eds.) (2001), *Climate Change 2001: The Scientific Basis—Contribution of Working Group I to the Third Assessment Report of the Intergovernmental Panel on Climate Change*, Cambridge Univ. Press, New York.

Jacob, D., et al. (1992), Summertime photochemistry of the troposphere at high northern latitudes, *J. Geophys. Res.*, *97*, 16,421–16,431.

Jaffe, D., I. Bertschi, L. Jaeglé, P. Novelli, J. S. Reid, H. Tanimoto, R. Vingarzan, and D. L. Westphal (2004), Long-range transport of Siberian biomass burning emissions and impact on surface ozone in western North America, *Geophys. Res. Lett.*, *31*, L16106, doi:10.1029/2004GL020093.

Jain, A. K., Z. Tao, X. Yang, and C. Gillespie (2006), Estimates of global biomass burning emissions for reactive greenhouse gases (CO, NMHCs, and NO$_x$) and CO$_2$, *J. Geophys. Res.*, *111*, D06304, doi:10.1029/2005JD006237.

Kasischke, E. S., and M. R. Turetsky (2006), Recent changes in the fire regime across the North American boreal region-Spatial and temporal patterns of burning across Canada and Alaska, *Geophys. Res. Lett.*, *33*, L09703, doi:10.1029/2006GL025677.

Kasischke, E. S., E. J. Hyer, P. C. Novelli, L. P. Bruhwiler, N. H. F. French, A. I. Suckhinin, J. H. Hewson, and B. J. Stocks (2005), Influences of boreal fire emissions on Northern Hemisphere atmospheric carbon and carbon monoxide, *Global Biogeochem. Cycles*, *19*, GB1012, doi:10.1029/2004GB002300.

Kleissl, J., et al. (2006), The occurrence of upslope flows at the Pico mountain-top observatory: A case study of orographic flows on a small, volcanic island, *J. Geophys. Res.*, doi:10.1029/2006JD007565, in press.

Kley, D., and M. McFarland (1980), Chemiluminescence detector for NO and NO$_2$, *Atmos. Technol.*, *12*, 63–69.

Kliner, D., B. Daube, J. Burley, and S. Wofsey (1997), Laboratory investigation of the catalytic reduction technique for measurement of atmospheric NO$_y$, *J. Geophys. Res.*, *102*, 10,759–10,776.

Kondo, Y., et al. (1997), Profiles and partitioning of reactive nitrogen over the Pacific Ocean in winter and early spring, *J. Geophys. Res.*, *102*, 28,405–28,424.

Lapina, K., R. E. Honrath, R. C. Owen, M. Val Martín, and G. Pfister (2006), Evidence of significant large-scale impacts of boreal fires on ozone levels in the midlatitude Northern Hemisphere free troposphere, *Geophys. Res. Lett.*, *33*, L10815, doi:10.1029/2006GL025878.

Li, Q., D. J. Jacob, J. W. Munger, R. M. Yantosca, and D. D. Parrish (2004), Export of NO$_y$ from the North American boundary layer: Reconciling aircraft observations and global model budgets, *J. Geophys. Res.*, *109*, D02313, doi:10.1029/2003JD004086.

Liang, J., L. W. Horowitz, D. J. Jacob, Y. Wang, A. M. Fiore, J. A. Logan, G. M. Gardner, and J. W. Munger (1998), Seasonal budgets of reactive nitrogen species and ozone over the United States and export fluxes to the global atmosphere, *J. Geophys. Res.*, *103*, 13,435–13,450.

Mauzerall, D. L., D. J. Jacob, S. M. Fan, J. D. Bradshaw, G. L. Gregory, G. W. Sachse, and D. R. Blake (1996), Origin of tropospheric ozone at remote high northern latitudes in summer, *J. Geophys. Res.*, *101*, 4175–4188.

Mauzerall, D. L., et al. (1998), Photochemistry in biomass burning plumes and implications for tropospheric ozone over the tropical South Atlantic, *J. Geophys. Res.*, *103*, 8401–8423.

McKeen, S. A., G. Wotawa, D. D. Parrish, J. S. Holloway, M. P. Buhr, G. Hbler, F. C. Fehsenfeld, and J. F. Meagher (2002), Ozone production from Canadian wildfires during June and July of 1995, *J. Geophys. Res.*, *107*(D14), 4192, doi:10.1029/2001JD000697.

Mollicone, D., H. Eva, and F. Achard (2006), Human role in Russian wild fires, *Nature*, *440*, 436–437, doi:10.1038/440436a.

Morris, G., et al. (2006), Alaskan and Canadian forest fires exacerbate ozone pollution over Houston, Texas, on 19 and 20 July 2004, *J. Geophys. Res.*, *111*, D24S03, doi:10.1029/2006JD007090.

Novelli, P. C., L. P. Steele, and P. P. Tans (1992), Mixing ratios of carbon monoxide in the troposphere, *J. Geophys. Res*, *97*, 20,731–20,750.

Novelli, P. C., K. A. Masarie, P. M. Lang, B. D. Hall, R. C. Myers, and J. W. Elkins (2003), Reanalysis of tropospheric CO trends: Effects of the

1997–1998 wildfires, *J. Geophys. Res.*, *108*(D15), 4464, doi:10.1029/2002JD003031.

Owen, R. C., O. R. Cooper, A. Stohl, and R. E. Honrath (2006), An analysis of the mechanisms of North American pollutant transport to the central North Atlantic lower free troposphere, *J. Geophys. Res.*, *111*, D23S58, doi:10.1029/2006JD007062.

Park, R. J., et al. (2005), Export efficiency of black carbon aerosol in continental outflow: Global implications, *J. Geophys. Res.*, *110*, D11205, doi:10.1029/2004JD005432.

Parrish, D. D., et al. (1990), Systematic variations in the concentration of NO$_x$ (NO plus NO$_2$) at Niwot Ridge, Colorado, *J. Geophys. Res.*, *95*, 1817–1836.

Parrish, D. D., J. S. Holloway, and F. C. Fehsenfeld (1994), Routine, continuous measurement of carbon monoxide with parts per billion precision, *Environ. Sci. Technol.*, *28*, 1615–1618.

Parrish, D. D., M. Trainer, J. S. Holloway, J. E. Yee, M. S. Warshawsky, F. C. Fehsenfeld, G. Forbes, and J. L. Moody (1998), Relationships between ozone and carbon monoxide at surface sites in the North Atlantic region, *J. Geophys. Res.*, *103*, 13,357–13,376.

Parrish, D. D., et al. (2004), Fraction and composition of NO$_y$ transported in air masses lofted from the North American boundary layer, *J. Geophys. Res.*, *109*, D09302, doi:10.1029/2003JD004226.

Peterson, M. C., and R. E. Honrath (1999), NO$_x$ and NO$_y$ over the northwestern North Atlantic: Measurements and measurement accuracy, *J. Geophys. Res.*, *104*, 11,695–11,707.

Pfister, G., P. G. Hess, L. K. Emmons, J.-F. Lamarque, C. Wiedinmyer, D. P. Edwards, G. Ptron, J. C. Gille, and G. W. Sachse (2005), Quantifying CO emissions from the 2004 Alaskan wildfires using MOPITT CO data, *Geophys. Res. Lett.*, *32*, L11809, doi:10.1029/2005GL022995.

Pfister, G., et al. (2006), Ozone production from boreal forest fire emissions, *J. Geophys. Res.*, doi:10.1029/2006JD007565, in press.

Reid, J. S., R. Koppmann, T. F. Eck, and D. P. Eleuterio (2005), A review of biomass burning emissions part II: Intensive physical properties of biomass burning particles, *Atmos. Chem. Phys.*, *5*, 799–825.

Ridley, B. A., and F. E. Grahek (1990), A small, low flow, high sensitivity reaction vessel for NO chemiluminescence detectors, *J. Atmos. Technol.*, *7*, 307–311.

Sandholm, S. T., et al. (1992), Summertime tropospheric observations related to N$_x$O$_y$ distributions and partitioning over Alaska: Arctic Boundary Layer Expedition 3A, *J. Geophys. Res.*, *97*(D15), 16,481–16,509.

Simmonds, P. G., A. J. Manning, R. G. Derwent, P. Ciais, M. Ramonet, V. Kazan, and D. Ryall (2005), A burning question. Can recent growth rate anomalies in the greenhouse gases be attributed to large-scale biomass burning events?, *Atmos. Environ.*, *39*, 2513–2517, doi:10.1016/j.atmosenv.2005.02.018.

Singh, H. B., et al. (1994), Summertime distribution of PAN and other reactive nitrogen species in the northern high-latitude atmosphere of eastern Canada, *J. Geophys. Res*, *99*, 1821–1835.

Stocks, B., et al. (1998), Climate change and forest fire potential in Russian and Canadian boreal forests, *Clim. Change*, *38*, 1–13.

Stohl, A., M. Trainer, T. B. Ryerson, J. S. Holloway, and D. D. Parrish (2002), Export of NOy from the North American boundary layer during 1996 and 1997 North Atlantic Regional Experiments, *J. Geophys. Res.*, *107*(D11), 4131, doi:10.1029/2001JD000519.

Stohl, A., C. Forster, A. Frank, P. Seibert, and G. Wotawa (2005), Technical note: The Lagrangian particle dispersion model FLEXPART version 6.2, *Atmos. Chem. Phys.*, *5*, 2461–2474.

Stohl, A., et al. (2006), Pan-Arctic enhancements of light absorbing aerosol concentrations due to North American boreal forest fires during summer 2004, *J. Geophys. Res.*, doi:10.1029/2006JD007216, in press.

Talbot, R. W. (1994), Summertime distribution and relations of reactive odd nitrogen species and NO$_y$ in the troposphere over Canada, *J. Geophys. Res.*, *99*, 1863–1885.

Tanimoto, H., Y. Kajii, J. Hirokawa, H. Akimoto, and N. P. Minko (2000), The atmospheric impact of boreal forest fires in far eastern Siberia on the seasonal variation of carbon monoxide: Observations at Rishiri, a northern remote island in Japan, *Geophys. Res. Lett.*, *27*(24), 4073–4076.

Wofsy, S. C., et al. (1992), Atmospheric chemistry in the Arctic and subarctic: Influence of natural fires, industrial emissions, and stratospheric inputs, *J. Geophys. Res.*, *97*, 16,731–16,746.

Wofsy, S. C., S.-M. Fan, D. R. Blake, J. D. Bradshaw, S. T. Sandholm, H. B. Singh, G. W. Sachse, and R. C. Harriss (1994), Factors influencing atmospheric composition over subarctic North America during summer, *J. Geophys. Res.*, *99*, 1887–1897.

Wotawa, G., and M. Trainer (2000), The influence of Canadian forest fires on pollutant concentrations in the United States, *Science*, *288*(5464), 324–328.

Yokelson, R. J., D. W. T. Griffith, and D. E. Ward (1996), Open-path fourier transform infrared studies of large-scale laboratory biomass fires, *J. Geophys. Res.*, *101*(D15), 21,067–21,080.

———————————

F. Barata and P. Fialho, Group of Chemistry and Physics of the Atmosphere, University of the Azores, Terra Chã PT-9701-851, Portugal.

R. E. Honrath, R. C. Owen, and M. Val Martín, Department of Civil and Environmental Engineering, Michigan Technological University, Houghton, MI 49931, USA. (mvalmart@mtu.edu)

G. Pfister, Atmospheric Chemistry Division, National Center for Atmospheric Research, Boulder, CO 80307, USA.